Universidade de Lisboa
Faculdade de Ciências
Departamento de Biologia Animal

narcissus is required for the correct establishment of left-right asymmetries in the zebrafish brain

Pedro Miguel Dias Henriques

Dissertation

Mestrado em Biologia Evolutiva e do Desenvolvimento

2013

Universidade de Lisboa
Faculdade de Ciências
Departamento de Biologia Animal

narcissus is required for the correct establishment of left-right asymmetries in the zebrafish brain

Pedro Miguel Dias Henriques

Dissertation

Mestrado em Biologia Evolutiva e do Desenvolvimento

External supervisor: Prof. Stephen Wilson
Internal supervisor: Prof. Sólveig Thorsteinsdóttir

2013

Man is all symmetry,
Full of proportions, one limb to another,
And all to all the world besides;
Each part may call the furthest brother,
For head with foot hath private amity,
And both with moons and tides.

In: Man *by* **George Herbert**

Acknowledgements

Um especial obrigado ao Steve Wilson, que, por poucas palavras, acreditou em mim, e a todos os (muitos!) elementos do laboratório, assimétricos ou não, que raramente recusaram partilhar uma *pint* e com quem espero partilhar muitas mais.

Um grande obrigado à minha não menor coordenadora Ana Faro, que me ensinou muito mais do que pensa, que estava normalmente presente quando as horas eram longas no laboratório e com quem posso partilhar hoje de uma boa amizade.

Um obrigado também à minha tia, que tornou esta e outras viagens possíveis, fazendo-me ver um pouquinho do mundo que ela já conhece, e à minha irmã, que desde pequeno me tem mostrado, consciente ou inconscientemente, um percurso pelo qual seguir.

Quero agradecer adicionalmente a todos os que me acompanharam e apoiaram até aqui, não só a nível profissional e académico, mas também a nível emocional. Aos familiares, aos amigos, aos amigos de circunstância, aos que se perderam, aos que nunca foram, aos que serão e a todos aqueles que me ensinaram, a bem ou a mal, a viver.

Acima de tudo quero agradecer aos meus pais, que por fruto do acaso se lembraram de me trazer ao mundo e me tentaram ensinar tudo o que sabiam, apesar das ocasionais resistências, e à minha avó e avô, que me educaram e me fizeram a pessoa que sou hoje. Amo-vos, apesar de não o dizer alto...

Abstract

The vertebrate brain is functionally and anatomically left-right (L-R) asymmetric, yet how these asymmetries arise and are maintained during development is still poorly understood. In zebrafish, the epithalamus comprises some of the most conspicuous asymmetries found in vertebrates, making it a valuable model to study their development. In it, left and right dorsal habenulae (dHb) develop differently in size, cytoarquitecture and axonal connectivity. Additionally, the parapineal organ migrates to the left side and exclusively projects to the left habenula (lHb), being required for the development of its molecular and subsequent cytoarchitectural left-sided identity. Several studies have shown that Nodal, Wnt and Notch signalling pathways have an important role in dHb asymmetric specification. However, how they interact with each other to achieve this is still largely unknown. Through a forward genetic screen, our lab has identified the *narcissus* mutation, which induces defects in the asymmetric specification of dHb neurons. Here, we show that in *narcissus* mutants, both habenulae display symmetric expression of some, but not all, lHb markers, and that the asymmetric afferent projections to the interpeduncular nucleus (IPN) and efferent innervation from the olfactory bulb and parapineal are disrupted. Additionally, both habenulae display significantly less BrdU incorporation in two tested timepoints, but asymmetric early neurogenesis still occurs.

Together, our findings demonstrate that *narcissus* is required for the correct specification of L-R asymmetries in the zebrafish brain and provide a valuable background for future studies to decipher its role in the establishment and maintenance of these asymmetries during embryonic development.

Keywords: *Brain asymmetry, Epithalamus, Habenula, Lateralization, Narcissus, Zebrafish*

Sumário

O cérebro é essencialmente assimétrico em termos anatómicos e funcionais, estando descritas assimetrias entre a esquerda e a direita no sistema nervoso de espécies representativas de praticamente todas as classes de vertebrados. De facto, há muito se sabe que várias funcionalidades se encontram extremamente lateralizadas no cérebro humano, como é o exemplo do processamento da linguagem, dominante no hemisfério esquerdo, e certas capacidades visuo-espaciais no hemisfério direito. Mais recentemente, vários estudos mostraram haver uma relação positiva entre cérebros pouco lateralizados e deficiências congénitas de linguagem, como no caso da dislexia, levando à hipótese de que estas poderão estar ligadas a problemas no estabelecimento de assimetrias durante o processo ontogénico. Apesar disto, pouco se sabe atualmente sobre como as assimetrias de esquerda-direita (E-D) aparecem e como são mantidas durante o desenvolvimento embrionário do sistema nervoso.

Há vários anos que o peixe-zebra tem provado ser um modelo valioso na área da biologia do desenvolvimento de vertebrados, muito devido ao seu bem caracterizado sistema genético, à facilidade de manipulação genética e celular e às suas propriedades óticas que facilitam técnicas de microscopia *in vivo*. No estudo do estabelecimento de assimetrias E-D, o peixe-zebra apresenta-se como particularmente útil. Neste organismo, a região cerebral do epitálamo, composta pelas habénulas e pelo complexo pineal, apresenta várias assimetrias entre a esquerda e a direita a nível citoarquitectónico, de expressão de genes e connectividade neuronal. A habénula dorsal do lado esquerdo é ligeiramente maior que a do lado direito, possuindo também uma maior concentração de neuropilo e expressão diferencial de genes. Esta diferença de expressão é na verdade tão acentuada, que permite a divisão dos núcleos da habénula nos subnúcleos lateral, demarcado pela expressão de *kctd12.1*, e medial, que expressa *kctd12.2*, e cujo tamanho é também proporcionalmente maior na esquerda e direita, respetivamente. Adicionalmente, o órgão parapineal, que origina de um subconjunto de células anteriores da glândula pineal, migra para o lado esquerdo e estabelece projeções axonais exclusivamente com a habénula

esquerda, sendo inclusivamente necessário para a correta especificação dos neurónios do sub-núcleo lateral nesse lado. Cada habénula projeta também diferencialmente para o núcleo interpeduncular, situado no mesencéfalo, onde a região dorsal e ventral é inervada preferencialmente pelas habénulas esquerda e direita, respetivamente.

Como se estabelecem estas assimetrias é ainda um tópico de grande debate. Sabe-se que a sinalização de Nodal, um dos primeiros eventos a quebrar a assimetria no embrião e necessária para o correto estabelecimento das assimetrias viscerais, possui também um papel crucial no estabelecimento das assimetrias epitamâmicas. Nodal é normalmente expresso no lado esquerdo do diencéfalo durante as primeiras fases do desenvolvimento, atuando como um *bias* no estabelecimento da lateralidade das assimetrias. De facto, vários estudos apontam para uma troca de informação entre a assimetria visceral e epitalâmica, sendo a primeira necessária para o estabelecimento da última através de uma interação mediada pela via de sinalização Wnt.

Vários estudos apontam na verdade para o requerimento de algumas das maiores vias de sinalização para o correto estabelecimento e manutenção de assimetrias no epitálamo. Para além de necessária para a quebra de assimetria inicial, a sinalização Wnt tem também um papel crucial na correta especificação dos sub-núcleos habenulares, pois a sua inibição através de tratamentos farmacológicos ou por mutações genéticas induz a diferenciação de um maior rácio de neurónios do sub-tipo dorsal lateral em ambas as habénulas, assumindo estas uma especificação característica de esquerda. Adicionalmente, a via de sinalização Notch parece estar envolvida na manutenção da cronologia do programa de neurogénese diferente entre esquerda e direita, mostrando-se essencial para a especificação diferencial dos neurónios dos dois lados. De facto, a maior parte dos neurónios do sub-núcleo lateral nasce por volta das 32 horas-pós-fertilização (hpf) enquanto que neurónios do sub-núcleo medial nascem mais tarde às 48 hpf. Apesar de várias hipóteses serem apontadas para esta assimetria, a mais plausível assenta na ideia de que na direita, uma ativação assimétrica da sinalização Notch leva a uma mais longa manutenção da população de células estaminais, inibindo assim a neurogénese nesse lado.

Apesar deste conhecimento, pouco se sabe em relação a como interagem

estas vias de sinalização para o estabelecimento de assimetrias no epitálamo. Para melhor compreender isto, o nosso laboratório realizou um *screening* genético para identificar mutações que resultem em problemas de assimetria epitalâmica. Um destes mutantes, *narcissus* (*nss*), é caracterizado pela bilateralidade de marcadores característicos da habénula esquerda, como *kctd12.1*, e sub-expressão de marcadores da habénula direita, como *kctd8*. Neste estudo, procurei caracterizar em maior detalhe o mutante *narcissus* e tentei identificar os mecanismos através dos quais este gera as perturbações de assimetria observadas.

Nos mutantes *narcissus*, todas as projeções aferentes e eferentes assimétricas para e das habénulas estão afetadas. Apesar da parapineal migrar corretamente para a esquerda, as suas projeções para a habénula esquerda possuem uma distribuição mais extensa do que em embriões controlo, cujas projeções tendem a acumularem-se em regiões mais próximas da habénula. Adicionalmente, a projeção assimétrica para a habénula direita, proveniente de células mitrais no bolbo olfactório e marcadas pela expressão do transgénico Tg(lhx2a:gap-YFP) estão completamente ausentes nos mutantes *narcissus*. Este defeito não será no entanto a provável causa da expressão simétrica de *kctd12.1*, pois a ablação seletiva destas projeções em embriões controlo antes da formação da enervação no epitálamo não revelou qualquer alteração de expressão de *kctd12.1* e do marcador da habenula direita *kctd8*. Inesperadamente, ambas as habénulas projetam também preferencialmente para a região ventral do núcleo interpeduncular, um fenótipo provavelmente causado por uma deficiência da sinalização de orientação axonial mediada por Nrp1a/Sema3D, intimamente responsável por esta conexão.

Ao contrário de outros mutantes onde marcadores da habénula esquerda são bilateralmente expressos, nos mutantes de *narcissus*, a expressão de Pku558b, que marca maioritariamente uma sub-população de neurónios na habénula do sub-tipo dorsal lateral, continua assimétrica aos 4 dias pós-fertilização (dpf). Por outro lado, a expressão de *kctd12.1* começa por ser assimétrica até 2 dpf, apenas adquirindo bilateralidade aos 3 dpf. Através da análise da data do nascimento dos neurónios dos diferentes sub-núcleos habenulares, identificámos que nos mutantes narcissus ocorre significativamente menos proliferação nas

habénulas às 32 e às 50 hpf, dois estádios do desenvolvimento em que a maioria dos neurónios dos dois sub-núcleos nascem. Este resultado sugere um mecanismo em mutantes onde uma diminuição da população de progenitores habenulares pode ser responsável pelos fenótipos observados. Apesar disto, a neurogénese assimétrica inicial mantém-se intacta nos mutantes *narcissus*.

Em conclusão, neste trabalho demonstrámos que *narcissus* é crucial para o desenvolvimento das assimetrias no epitálamo do peixe-zebra, providenciando um valioso conhecimento para o decifrar do seu papel no estabelecimento e manutenção destas assimetrias em estudos futuros.

Palavras chave: *Assimetria cerebral, Epitálamo, Habenula, Lateralização, Narcissus, Peixe-zebra*

Contents

List of Figures

Nomenclature

DDC Dorsal Diencephalic Conduction system

dHb Dorsal Habenula

dHbL Lateral sub-nucleus of the Dorsal Habenula

dHbM Medial sub-nucleus of the Dorsal Habenula

dIPN Dorsal Interpeduncular Nucleus

dpf Days-post-fertilization

hpf Hours-post-fertilization

L Left

LHb Lateral Habenula

lHb Left Habenula

MHb Medial Habenula

OB Olfactory Bulb

R Right

rHb Right Habenula

vHb Ventral Habenula

vIPN Ventral Interpeduncular Nucleus

Chapter 1

Introduction

1.1 Brain laterality: from genes to behaviour

George Herbert wasn't wrong to praise man's symmetry, for it does indeed seem to be the default condition in the biological world. But beneath this superficial view, it is stunning to find that left-right (L-R) asymmetries not only exist, but are extremely widespread across phyla, conferring an advantage even in the presence of a seemingly symmetrical world. This is indeed true for our internal organs, such as the heart, lungs, stomach and liver, which are asymmetrically arranged, most likely as a way for a more efficient packaging. Not so differently, in the nervous system, both structural and functional L-R asymmetries have been described from roundworms to humans where they've been shown to influence physiology, cognition and animal behaviour (Hobert et al., 2002; Frasnelli et al., 2012; Vallortigara and Rogers, 2005).

In humans, one of the most obvious functional asymmetries is hand dominance, or handedness. Approximately 90% of the world population is dominant for the right-hand, meaning that in these, most tasks requiring hand manipulation are best performed with the right hand than with the left one (Corballis, 2009). Although this may suggest hand structure to be different between sides, it is in fact a difference in skill that is responsible for this dominance, reflecting a cerebral asymmetry, rather than a mechanical one, to be its cause. But despite handedness being known for centuries, interest in brain lateralization was only

sparked in the mid- nineteenth century, when Paul Broca, with the observation that patients with left hemispheric damage were usually accompanied by language impairments, discovered that language processing in humans is dominant to the left hemisphere (Broca, 1965). Several years later, by studying the so-called split-brain patients, in whom the *corpus callosum* which connects the two brain hemispheres had been surgically severed to control the spread of epileptic seizures, researchers were able to pave the way to the discovery of many other brain functional lateralizations, allowing them to separately stimulate each hemisphere and record its functional output (Gazzaniga, 2005; Wolman, 2012).

Functional brain lateralization is thought to arise from differences in the anatomical structure and neuronal circuitry between hemispheres. A century after Broca's discovery, Geschwind and Levitsky conclusively demonstrated that a significant L-R size asymmetry existed in the *planum temporale*, a region associated with language processing and handedness (Geschwind and Levitsky, 1968). More recently, structural magnetic resonance imaging (MRI) studies allowed the visualization and quantification of other anatomical brain asymmetries (Figure 1.1). For example, the right frontal lobe *petalia* and the left occipital *petalia*, impressions left on the inner surface of the skull by protrusions of one hemisphere relative to the other, were shown to be more pronounced in right-handed individuals (Kertesz et al., 1986). Also, Good and colleagues found that males have a greater leftward asymmetry in the *planum temporale* and *Heschl's gyrus*, when compared to females (Good et al., 2001), following the idea that males possess a more asymmetrical brain than females, a feature thought to underlie differences in motor, visuospatial skills and linguistic performance between genders (Hiscock et al., 1994).

Although much is known about human brain lateralization, it is far from true that we are the only specie that exhibits such feature. To date, an increasing amount of studies strongly argue for functional lateralization to be a highly conserved and universal feature of the vertebrate brain and, in some of these, to be associated with anatomical and molecular asymmetries (Bisazza et al., 1998; Vallortigara and Rogers, 2005) (Table 1.1). Toads, for example, are more likely to flee away from a predator if it appears in their left visual hemifield (Lippolis et al., 2002). Similarly, many species of teleosts preferentially use the right eye

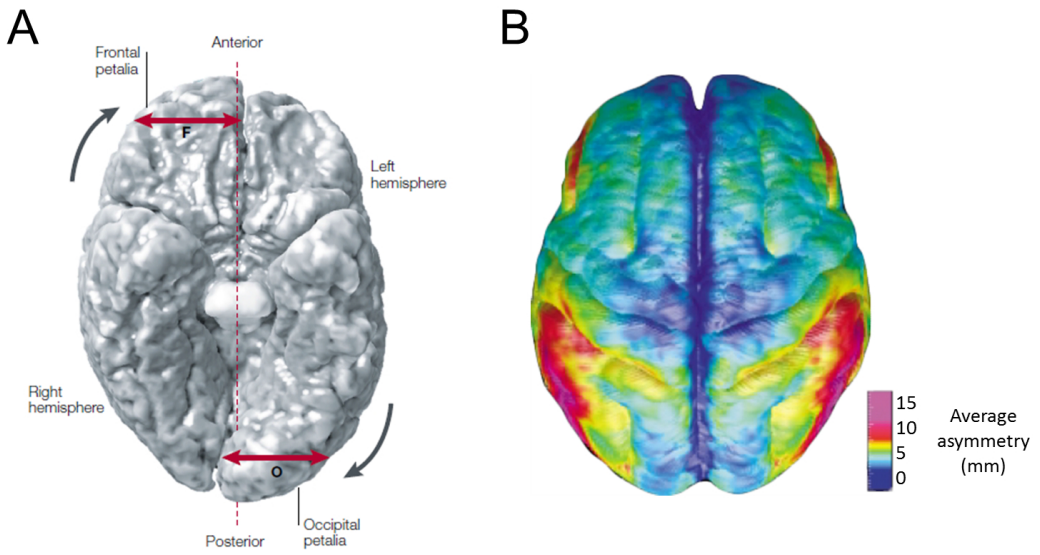

Figure 1.1: **Structural L-R asymmetries in the human brain. A,** Three-dimensional rendering of a MRI scan of a human brain showing marked and artificially exaggerated L-R asymmetries. Prominent differences in the protrusions of both hemispheres and widths of the frontal (F) and occipital (O) lobes are observed. Also, the left occipital lobe spreads across the midline and skews the interhemispheric fissure in a rightward direction. **B,** Map of surface brain asymmetries produced by averaging of several individual MRI scans. Prominent asymmetries can be identified in the Broca's anterior speech area and in language regions surrounding the Sylvian fissure. Image in A is from dorsal and in B from ventral perspective. Images adapted from (Toga and Thompson, 2003).

Left hemisphere	**Right Hemisphere**
Considered responses: Able to inhibit responding while deciding between alternative responses; Visuo-spatial analysis centered on local features	*Rapid, species-typical responses; Visuo-spatial analysis centered on relational properties of the spatial layout*
Prey discrimination and catching (fish, toads)	Predator detection (fish, chicks)
Foraging with discrimination and/or manipulation of food items (birds)	Predator escape (frog tadpoles, fish, toads, chicks, dunnarts)
Approach and manipulation of objects (birds, monkeys, apes)	Neurochemical changes with predator stress (rats, cats)
Inhibition of aggression (chicks, humans)	Avoidance/withdrawal (monkeys, apes, humans)
Inhibition of intense emotions, especially negative emotions (humans)	Fear (chicks, rats)
Recognition of categories/attention to large changes (birds, rats)	Aggression (toads, lizards, chicks, monkeys)
Recognition of species-typical vocalizations (birds, mice, some monkeys, humans for speech)	Courtship and copulatory behaviour (newts, birds)
Attention to landmarks (birds)	Contact/monitoring of conspecifics (fish, tadpoles)
Attention to local cues (birds, monkeys, humans)	Expression of intense emotions (monkeys, apes, humans)
	Recognition /analysis of faces (sheep, monkeys, humans)
	Recognition of individual conspecifics (chicks)
	Spatial cognition (birds, rats, humans)
	Attention to global cues (chicks, monkeys, humans)

Table 1.1: **Summary of some reported lateralized functions in different species.** Left and right columns represent functions dominant to the left or right cerebral hemisphere respectively. Adapted from (Vallortigara and Rogers, 2005)

when approaching a possible predator, while prefer to examine conspecifics with the left eye (Miklósi et al., 2001, 1997).

Aggressiveness towards conspecifics also seem to be strongly lateralized to the left hemifield in many species, while prey catching and foraging responses have a rightward bias, particularly when there is need for considerate discrimination between stimuli or careful manoeuvring of objects (Vallortigara and Rogers, 2005). As left and right sensory hemifields are controlled by their contralateral cerebral hemispheres, these findings argue for a right hemispheric control of more emotional and rapid responses and a left control of more considered ones. In agreement with this, impairments of the left hemisphere in humans, forcing the right one to take control, leads to the expression of more intense, and sometimes aggressive, emotions (Nestor and Safer, 1990).

Why is it that so many species exhibit functional brain lateralization? In a physical world that is indifferent to left or right, it seems disadvantageous to have, for example, fleeing responses lateralized to one hemifield, as it is as likely for a predator to appear from either the left or the right. One theory argues that an asymmetrical brain is able to increase neuronal capacity, as the specialization of a particular function to one side leaves the other one free to perform other tasks, thereby allowing the brain to perform parallel processing more efficiently (Levy, 1977). Supporting this hypothesis, Rogers and colleagues found that chicks that have strong lateralized brains are more able to simultaneously perform pecking (left hemisphere dominant) and predator detection (right hemisphere dominant) tasks (Rogers et al., 2004). Not contrary to this view, a lateralized brain might also be a way to avoid inter-hemispheric competition for similar tasks, and to avoid the simultaneous appearance of incompatible responses (Vallortigara and Andrew, 1991; Vallortigara, 2000). This is particularly important in species that exhibit a great independence of left and right hemifields, as failure to suppress one response induced by two similar but contralateral stimuli might have disastrous consequences (Wallman and Pettigrew, 1985).

If a more asymmetrical brain seems to be an advantage, at least at the individual level, is it possible to attribute the cause of disabilities in strongly lateralized functions, such as language (left) and visuo-spatial analysis (right), to defects in brain lateralization? Several studies, starting almost a decade ago, have suggested that language literacy impairments in humans, such as dyslexia and Specific Language Impairment (SLI) are linked to poorly lateralized brains (Bishop, 2013). More recently, this link was further supported with the improvement of neuroimaging techniques such functional Transcranial Doppler Ultrasound (fTCD) and functional Magnetic Resonance (fMRI) (Knecht et al., 1998; Badcock et al., 2012). As both language impairments and brain laterality are heritable ($\pm$70% for dyslexia), one can infer that they might be genetically linked. In this view, several models of association can be deduced: (1) genes might influence language impairments by being directly linked with laterality, while the latter is responsible for the impairments (endophenotype model); or (2) genes affect both language and laterality without being a relation between the last two (pleitropy model). Studies in twins and genetic variants in genes linked to language impairments have

uncovered a correlation between laterality and these impairments, but inconsistencies between studies cast doubt on their robustness (Bishop, 2013). Where found, correlations were usually of low effect thus arguing against the endophenotype model. Nonetheless, polymorphisms in several genes, such as FOXP2 and CNTNAP2, show a promising link with brain structural and functional asymmetries, arguing, at least in part, for a genetic predisposition to language literacy impairments (Kos et al., 2012; Pinel et al., 2012).

1.2 The epithalamus and the dorsal diencephalic conduction system

Some of the most conspicuous and best described central nervous system asymmetries of vertebrates can be found in the epithalamus. This structure arises during embryonic development through a major subdivision of the diencephalon and is constituted by two sets of neuronal conglomerates, the habenular and pineal complexes (Concha and Wilson, 2001). The pineal complex itself is comprised of the medially located pineal organ (or epiphysis) and the associated parapineal organ (fish), frontal organ (amphibians) or parietal eye (reptiles). With the exception of amphibians, the parapineal sends axonal projections exclusively to the left habenula in lampreys, lizards and teleosts, while also positioning itself to the left side of the midline in teleosts. The pineal organ function has long been established as to regulate circadian rhythmicity in response to light/dark conditions through the synthesis of melatonin (Wurtman et al., 1964). By contrast, the function of the parapineal organ remains largely unknown, although the presence of poorly developed photoreceptors might indicate a rudimentary light sensitive function (Tamotsu et al., 1990).

The habenular complex is composed of bilaterally paired nuclei, connected to each other through the habenular commissure, and functions as a relay unit in one of the two major pathways that interconnects the limbic forebrain to the midbrain, known as the dorsal diencephalic conduction (DDC) system (Figure 1.2). It primarily receives inputs from several telencephalic nuclei through an axonal fibre bundle know as *stria medullaris*, projecting afterwards through the

fasciculus retroflexus to several targets in the midbrain/hindbrain (Bianco and Wilson, 2009). Each habenular nuclei is further subdivided into medial (MHb) and lateral (LHb) nuclei, with distinct neural connectivity. The LHb establishes efferent projections into dopaminergic centres in the midbrain, like the ventral tegmental area (VTA) and the substantia nigra pars compacta (SNc), but also into serotonin releasing centres such as the dorsal and median raphe nuclei. The MHb, however, projects almost exclusively to the interpeduncular nucleus (IPN) in the midbrain, a connection evolutionary conserved from lamprey to humans (Aizawa, 2012), which is in turn also connected to the raphe nuclei.

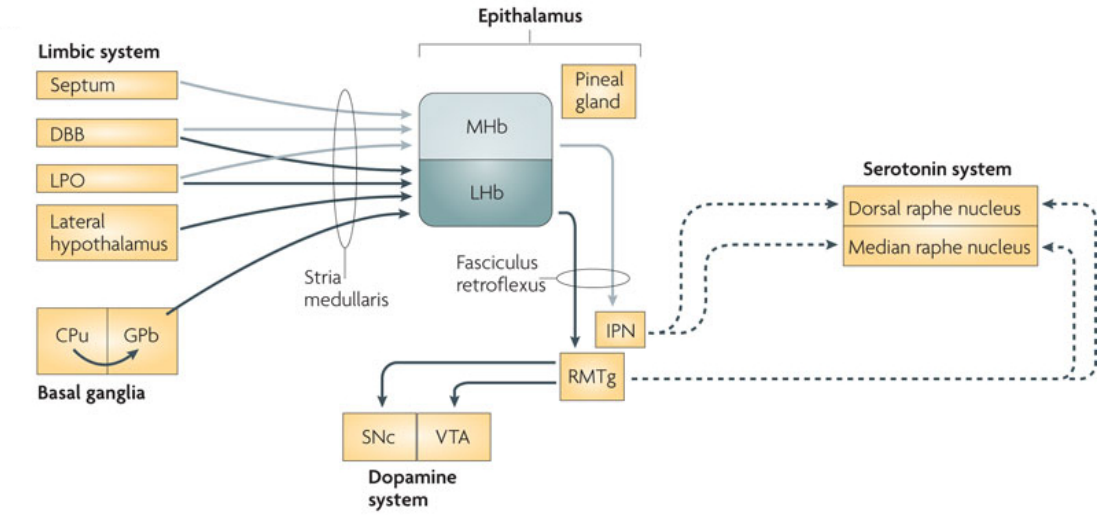

Figure 1.2: **Diagram of the afferent and efferent connectivity of the mammalian habenula.** The MHb, LHb and pineal gland comprise the epithalamus. The MHb receives inputs mainly from the limbic system and sends outputs to the interpeduncular nucleus (IPN), which projects to the raphe nuclei. The LHb receives inputs mainly from the basal ganglia and sends outputs to the brain structures that contain dopaminergic neurons and serotonergic neurons, partly through the rostromedial tegmental nucleus (RMTg). Light and dark grey lines indicate the axonal connections associated with the MHb and LHb, respectively. CPu, caudate and putamen; DBB, diagonal band of Broca; GPb, border region of the globus pallidus; LPO, lateral preoptic area; SNc, substantia nigra pars compacta; VTA, ventral tegmental area. Adapted from (Hikosaka, 2010)

.

Several recent studies have determined the mammalian habenula to be involved in a diverse range of cerebral functions such as reward-based decision making, pain avoidance, control of sleep and stress responses, and to be linked to psychiatric disorders such as major depression, drug-induced psychosis and schizophrenia (Hikosaka, 2010). In both humans and macaque monkeys, the LHb has been shown to indirectly inhibit dopamine release by being active when an individual is faced with a smaller-than-expected reward, thereby driving reinforcement learning. LHb neurons were also shown to be active following prolonged stress-inducing stimuli in rats and monkeys, leading to motor suppression and lack of motivation (leaned helplessness), and also to be hyperactive in both humans with major depression disorder (MDD) and animal models of the condition (Matsumoto and Hikosaka, 2007; Ullsperger and von Cramon, 2003; Caldecott-Hazard et al., 1988; Li et al., 2013).

Studies unravelling the function of MHb are sparse in mammals due to the small size and inaccessibility of this structure. Despite this, MHb and IPN neurons were found to have increased activity in MDD model rats and to modulate nicotine withdrawal symptoms in mice (Shumake et al., 2003). In the latter, responses are mediated through nicotine acetylcholine receptors, which are highly concentrated in MHb neurons (Salas et al., 2009). The administration of high doses of nicotine also causes massive degeneration almost exclusively to these regions (Carlson et al., 2001). A recent study in zebrafish has also showed that the lateral dorsal habenula (dHbL), a subdivision of the MHb homolog in fish, is implicated in experience-dependent fear responses. When these neurons were selectively inactivated by tetanus toxin, both treated and non-treated fish exhibited a freezing response when first exposed to an aversive stimulus. But while non-treated fish showed enhanced flight behaviours after several exposures to the stimulus, dHbL-silenced fish showed a persistent freezing response, suggesting that the dHb mediates stress-response behaviours in this organism (Agetsuma et al., 2010).

Habenular L-R asymmetries, whether in size, neuronal organization, connectivity, neurochemistry or gene expression, have been documented in virtually all classes of vertebrates. In mammals and birds however, few accounts of habenula L-R asymmetries have been reported. In chicks, the right habenula is enlarged in

males, but not in females, a difference mediated by the levels of testosterone during development (Gurusinghe et al., 1986). Studies performed in albino rats and mice also showed that both have a L-R size asymmetry in the habenula, but the laterality is not concordant between them, adding to the view that asymmetry *per se*, rather than laterality, is important for habenular function (Wree et al., 1981; Zilles et al., 1976). Despite the rare observations in mammals and birds, it is important to note that many studies have only focused on size differences, and so, less obvious asymmetries, particularly in terms of neuronal connectivity and specificity might have gone under the radar.

1.3 Zebrafish as a model to study brain L-R asymmetries *or* ***How to build an asymmetric brain***

Structural and functional L-R brain asymmetries are thought to be highly dependent on the establishment of molecular and anatomical asymmetries during the embryonic development of the central nervous system. In recent years, the epithalamus of zebrafish (*Danio rerio*) has been championed as a model for studying the development of brain lateralisation because of its overt neuroanatomical asymmetries, suitability for *in vivo* imaging and amenability to genetic manipulation. Furthermore, it is the only vertebrate model to date in which asymmetric gene expression in the brain has been directly linked to the development of asymmetric morphology.

The zebrafish habenular nuclei are comprised of dorsal habenular (dHb) and ventral habenular nuclei (vHb), homologous to the mammalian MHb and LHb, respectively (Amo et al., 2010). The dHb displays overt left-right asymmetries, with distinct ratios of neuron subtypes, as defined by molecular markers expression and neuronal connectivity (Figure 1.3). These differences in cytoarchitecture are so relevant that justify further subdividing the dHb into lateral (dHbL) and medial (dHbM) sub-nuclei. While the dHbL is significantly larger than the dHbM on the left side, on the right side this difference is reversed (Gamse et al., 2005). Also, the dHbL specifically expresses the *potassium channel tetramerisation do-*

main containing 12.1 (*kctd12.1*) gene and predominantly innervates the dorsal part of the IPN (dIPN) while the dHbM is characterized by *potassium channel tetramerisation domain containing 12.2* (*kctd12.2*) expression and predominantly innervates the ventral IPN (vIPN) (Aizawa et al., 2005). Several other genes have been found to be expressed in different sub-domains of the habenula, some also presenting L-R asymmetries, suggesting the existence of more than two habenular sub-nuclei in zebrafish (Gamse et al., 2005). Indeed, 15 different sub-nuclei have been identified in the rat habenula based on cell morphology, immunoreactivity and expression of marker genes for known neurotransmitters (Andres et al., 1999; Geisler et al., 2003; Aizawa, 2012). Adding to the L-R asymmetries of the zebrafish habenulae, the parapineal, an accessory organ to the pineal, is also displaced to the left side of the brain in 95% of zebrafish larvae and sends axonal projections only to the left habenula (Gamse et al., 2003).

How these differences arise during development has been an expanding topic of research in recent years (Figure 1.4). It was particularly sparked by the finding that the transforming-growth-factor β (TGF-β) family member Nodal, which acts as a L-R determinant of the body axis and is ultimately responsible for the asymmetric disposition of the internal organs, is also determinant is establishing brain L-R asymmetries. Around 24 hours-post-fertilization (hpf), *nodal-related 2*(*ndr2*)/*cyclops* (which encodes a Nodal ligand) is expressed on the left side of the presumptive epithalamus, inducing on that side the activation of the Nodal inhibitor *lefty1* and *pitx2c* (Liang et al., 2000; Concha et al., 2000). Interestingly, the left-sided activation of Nodal in the epithalamus seems to be dependent on the mechanisms that govern L-R asymmetry in the viscera. Mutants of *southpaw* (*spaw*), which encodes for a LPM expressing Nodal ligand, exhibit both epithalamic and visceral L-R deficiencies (Long et al., 2003). Furthermore, early epithalamic asymmetry seems to be dependent on an interaction between Nodal and Wnt signalling, as indicated by the bilateral activation of Nodal signalling in *masterblind* embryos, where Wnt/β-catenin signalling is overactivated. At around 11 hpf, bilateral Wnt signalling indirectly represses Nodal on both sides of the epithalamus by interacting with Six3 (Carl et al., 2007). This repression is later overcome on the left side by an interaction with the left LPM expression of *spaw*, through a mechanisms not yet understood (Long et al., 2003).

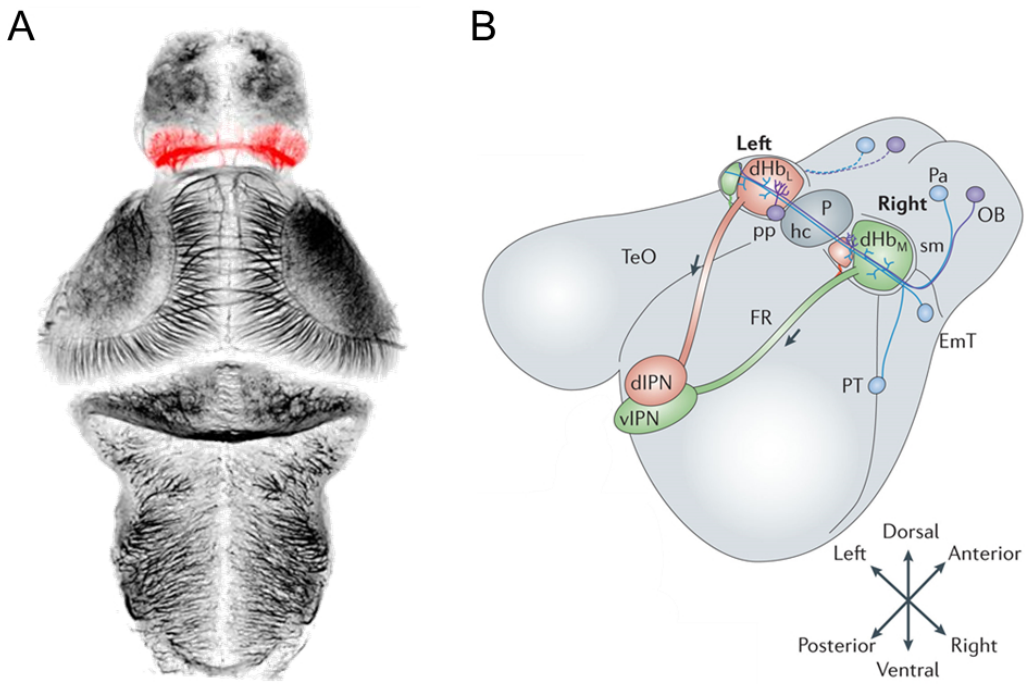

Figure 1.3: **Asymmetric circuitry in the zebrafish epithalamus. A,** Neuronal circuitry in the zebrafish brain as evidenced by acetylated α-tubulin staining, used to visualise neuronal cell bodies and their axons. The habenular domain is pseudocoloured in red. **B,** Lateral (dHbL) and medial (dHbM) dorsal habenulae are asymmetrically enlarged in the epithalamus and mostly send efferent projections to the dorsal (dIPN) and ventral (vIPN) interpeduncular nucleus, respectively. The parapineal (pp) also only innervates the dHbL and some neurons originating in the olfactory bulb (OB) and pallium (Pa) specifically send projections to the dHbM and dHbL, respectively. EmT, eminentia thalami; FR, fasciculus retroflexus; hc, habenula commissure; P, pineal; PT, posterior tuberculum; sm, stria medullaris; TeO, optic tectum. Figure 2A: Kate Turner. Figure 2B adapted from (Concha et al., 2012)

In the absence of unilateral Nodal signalling, either by mutations in the pathway genes or by treatment with inhibitory drugs, L-R asymmetries still develop but their laterality is randomized. This suggests that unilateral Nodal signalling in the epithalamus is not required for the establishment of L-R asymmetries *per se*, but rather introduces a bias in their laterality (Concha et al., 2000). Recently, however, this view has been argued against by the finding that the presence of Nodal signalling is required for asymmetric neurogenesis of early-born habenular precursors (Roussigné et al., 2009). Indeed, Aizawa and colleagues have elegantly showed that left and right habenular neurons are specified with different timings, so while dHbL neurons are primarily born at around 32 hpf, most dHbM neurons are born at 48 hpf (Aizawa et al., 2007). They also showed that neurogenesis timing was dependent on Notch signalling activation, as overexpression of the notch intracellular domain (NICD) at either 32 or 48 hpf was able to completely abolish *kctd12.1* and *kctd12.2* expression, respectively. This led to the hypothesis that Notch modulates habenular neurogenic fates by inducing cells to remain in a proliferative state on the right side for a longer period of time, although until now, no concrete evidence of asymmetric Notch signalling activity in the epithalamus has been reported. Recent studies in chickens indicated that Notch signalling functions as an upstream signal to induce Nodal in the left side of Hensen's node prior to neurogenesis (Raya et al., 2003, 2004). However, in *mindbomb* (*mib*) mutant zebrafish embryos, where Notch signalling is absent (and which display bilateral, absent or reversed Nodal signalling in half the embryos) bilateral left-sided character habenular neurons still develop, independently of the pattern of Nodal expression, suggesting that in the zebrafish diencephalon Nodal may act upstream of Notch to modulate asymmetric neurogenesis (Aizawa et al., 2007).

Despite Nodal being the first known gene to be asymmetrically expressed in the zebrafish brain, the parapineal migration is the first anatomical evidence of L-R asymmetry in the epithalamus. After delaminating from the anterior part of the epiphysis, it starts a leftward migration at 28-36 hpf, undergoing afterwards a series of movements that culminate in its final position at the left, ventral and posterior side of the pineal. Fgf8 has been shown to be both required and sufficient for parapineal cells to begin migrating, acting as a chemotactic signal that along with Nodal left-sided expression ensures a leftward migratory "choice"

(Regan et al., 2009). The parapineal is also essential to specify the left-sided identity of the left habenular nucleus. Laser-ablation of the parapineal primordium prior to its migration reduces the asymmetry of the habenulae, with both sides developing a largely right phenotype with respect to gene expression and projections to IPN (Gamse et al., 2003). How the parapineal specifies the identity of habenular neurons is still unknown, but one hypothesis is that it may act to modulate signalling pathways known to be involved in controlling habenular neuronal identity, such as Notch and Wnt. Wnt signalling seems indeed to be required for dHb asymmetric fate specification. In *masterblind/axin1* mutants, where Wnt signalling is overactivated, both habenulae develop with right-sided character but the parapineal's leftward migration and its axonal projections to the left habenula are not disturbed (Carl et al., 2007). Conversely, Wnt signalling inhibition by drugs during the period that most dHbL neurons are born (32-48 hpf) lead both habenulae nuclei to develop left-sided character (Hüsken U. and Carl M.; personal communication). Furthermore, mutants for *tcf7l2*, a downstream effector of the canonical Wnt pathway, also show bilateral left-sided dHb character, even when the parapineal is ablated. These observations suggest that the parapineal may act by repressing tcf7l2-dependent Wnt signalling on the left side and thereby promoting dHbL differentiation on that side (Hüsken U. and Carl M.; personal communication). Another explanation is that the parapineal may amplify existing L-R differences in neurogenesis by repressing the activity of Notch signalling on the left side. Despite these observations, further studies are required to provide a convincing explanation in this matter.

The habenular L-R structural and molecular asymmetries predict that they mediate functional lateralization, most likely through an asymmetric modulation of its efferent targets. Zebrafish show a right or left eye preference when approaching an object that is new or has been seen before respectively (Miklósi and Andrew, 1999; Miklósi et al., 1997), and this preference was shown to be reversed in larvae that have reversed epithalamic asymmetry (Barth et al., 2005). They were also shown to have left-sided odour-preference behaviour in adults, but not in juveniles, and left, but not right, olfactory deprivation led to a reduction in neuronal activity in the left dHb (Kishimoto et al., 2013). Light stimulation mediated by the retina, but not by the parapineal, also seems to preferentially

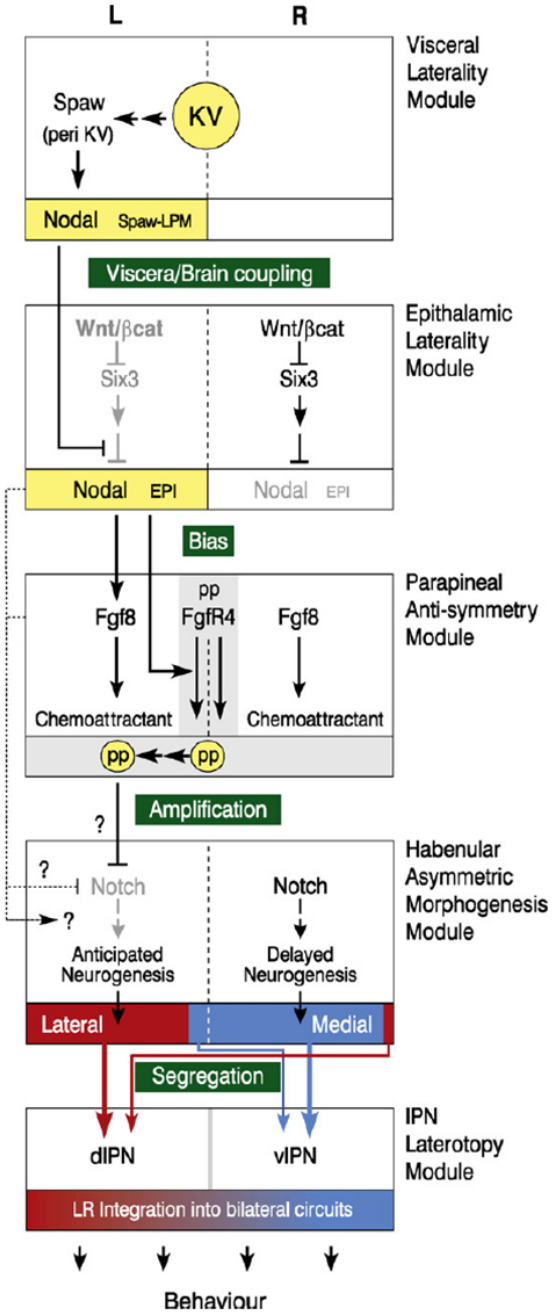

Figure 1.4: **Current model of the development of epithalamic asymmetry during embryonic development in zebrafish.** The different processes are represented in a modular disposition where each module (box) has an input (top), an internal process (inside) and an output signal (bottom). The interaction between developmental modules culminates in a behavioural output. See main text for further details. d/vIPN, dorsal and ventral interpeduncular nucleus; EPI, epithalamus; KV, kupffer's vesicle; L, left; Lateral, lateral dorsal habenula; LPM, lateral plate mesoderm; Medial, medial dorsal habenula; pp, parapineal; R, right. Adapted from (Concha et al., 2009)

induce neuronal activity in the left dHb and dIPN, while odour stimulation induces activity in the right dHb and vIPN (Droesti E. and Wilson S.; personal communication). These accounts strongly argue for a major role of the zebrafish asymmetric epithalamus in the modulation of lateralized behaviours.

1.4 the *narcissus* mutant

Despite the growing understanding on how L-R asymmetries arise during embryonic development, little is known on how the different cellular and molecular mechanisms interact to give rise to and maintain them. In an attempt to better understand these interactions, our team conducted an N-ethyl-N-nitrosourea (ENU)-induced forward genetic screen in zebrafish to identify phenotypes with disrupted habenular, but normal visceral, L-R asymmetries. One fully penetrant recessive mutation was identified, *narcissus* (*nss*), in which the visceral asymmetry is normal but both the left and right habenulae display left-sided character (Figure 1.5). Interestingly, left-sided expression of the Nodal target, *pitx2*, in the diencephalon is unaffected in *nss* mutants (Figure 1.5A-B).

Preliminary analysis also showed that in *nss* mutants, the parapineal correctly migrates to the left side, as shown by *otx5* expression, a pineal and parapineal marker (Gamse et al., 2002) (Figure 1.5C-D). Contrary to wild-type, however, *kctd12.1* is bilaterally expressed and all right-sided markers, *kctd8*, *cntn2* and *vchat* are strongly reduced in the left dHb, but also on the right at 4 dpf (Figure 1.5I-J,M-R). Interestingly enough, *kctd12.1* is still asymmetrically expressed until 2 dpf, only becoming bilateral at 3 dpf (Figure 1.5E-H). Also, the pku558 transgene, which labels a dorsal population of dHbL neurons in wild-type (Hüsken U. and Carl M.; personal communication), is also asymmetrically expressed in *nss* mutants at 4 dpf (Figure 1.5K-L). Furthermore, and contrary to expected, the left-sided asymmetry in the habenular neuropil observed in wild-type is also found in *nss* mutants (Figure 1.5U-V), and the expression of the ventral habenula marker *kiss1* is downregulated in mutants (Figure 1.5S-T).

In this work I undertook a further characterization of the *nss* mutant phenotype to understand when and how does the mutated gene act to give rise to L-R asymmetries in the zebrafish epithalamus. I discovered that in *nss* mutants,

the asymmetric axonal afferents and efferents to and from the habenulae are disrupted. I also found that less BrdU incorporation is observed in both habenulae of *nss* mutants at both 32 and 50 hpf and that both habenulae are also smaller in size in comparison to wild-type siblings. In addition, these phenotypes do not seem to be a consequence of absent asymmetric innervation from olfactory bulb mitral cells to the right habenula, nor disruptive Wnt signalling during the first neurogenic wave.

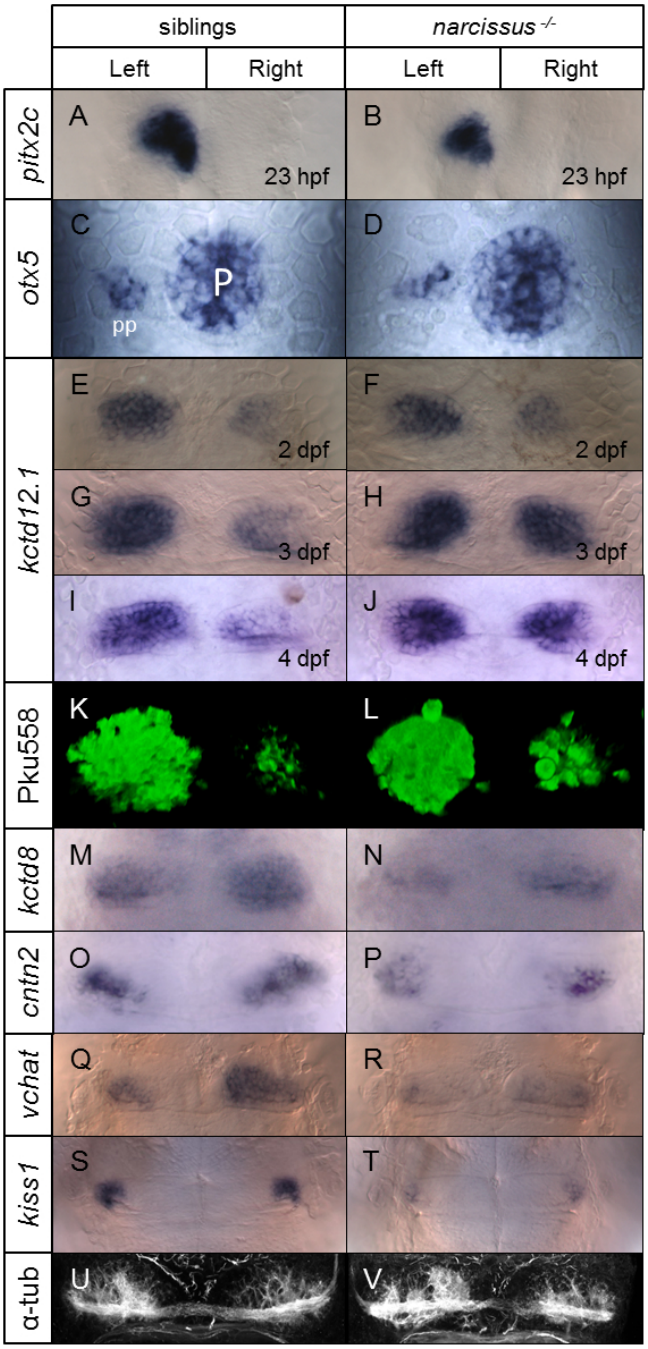

Figure 1.5: ***narcissus*** **mutants have disrupted L-R asymmetry of the habenular nuclei. A-V,** *In situ* hybridization or immunohistochemistry of genetic markers for the **A-B,** Nodal signalling pathway, **C-D,** pineal and parapineal, **E-L,** left-side dominant habenular subnuclei, **M-R,** right-side dominant habenular subnuclei, **S-T,** ventral habenula and **U-V,** habenular neuropil. α-tub, acetylated α-tubulin; P, pineal; pp, parapineal. All embryos are at 4 dpf unless expressed otherwise.

Chapter 2

Material and Methods

2.1 Zebrafish lines and maintenance

Zebrafish strains were maintained and bred according to standard procedures (Westerfield, 2000). Embryos were maintained in a 14/10 hour light/dark cycle, as light has been shown to influence the timing of habenular neurogenesis (de Borsetti et al., 2011) and 0.002% phenylthiourea (PTU) was added to the fish water from 12 hpf to inhibit pigment formation.

Wild-type siblings and homozygous *nss* mutant embryos were obtained by incross of nss$^{+/-}$, nss$^{+/-}$; Tg(FoxD3:GFP), nss$^{+/-}$; Tg(lhx2a:gap-YFP), nss$^{+/-}$; Tg(ClnB:GFP) or nss$^{+/-}$; Tg(Pku558:GFP) transgenic fish. Mutants were either phenotypically identified by *in situ* hybridization using a cocktail of *kctd12.1*, *fabp1a* and *trypsin* probes or by a genotyping assay by PCR amplification using the z9321 genetic marker (GenBank: G40766.1) which co-segregates with the *nss* mutation. The Tg(lhx2a:gap-YFP) fish line was used for the axotomy experiments. Efficiency of Wnt agonist/antagonist pharmacological treatments were assessed in Tg(7Xtcf-siam:GFP)^{ia4}.

2.2 Whole-mount *in situ* hybridization and immunohistochemistry

In situ hybridization and immunostaining was performed as previously described (Thisse and Thisse, 2008; Macdonald, 1999). For fluorescent *in situ* hybridization coupled with immunohistochemistry, *in situ* hybridization was performed first using fast red TR/Naphtol tablets (Sigma) following manufacturer's protocol.

In situ anti-sense probes for *kctd12.1* and *kctd8* (Gamse et al., 2005), *fabp1a* (Her et al., 2003) and *trypsin* (Biemar et al., 2001) were synthesised as described (Thisse and Thisse, 2008). DNA templates for *sema5a*, *plexin B3* and *nrp1a* anti-sense probes were prepared by PCR amplification from cDNA libraries (prepared from 24, 50 and 30 hpf embryos) using the following primers: *sema5a* (FW: 5'-CAG TCG TGG GAA ATC AGA GG-3'; RV: 5'-TCC ATG AAA TAC GGC ACA GG-3'), *plexin B3* (FW: 5'-ATT GCT CAA CCG TGA AAC TG-3'; RV: 5'-CCT TCC TGG TCC TTG TTT CT-3'), *nrp1a* (FW: 5'-ATT ACT CGT CTA TTT CGC GGA ACT GC-3'; RV: 5'-ACAGAGCCTTGTCCTCCTCCAATC-3'). PCR fragments were purified from 1% agarose gel (QIAquick®PCR Purification Kit, QIAGEN) and cloned into the expression vector pCRII-TOPO (TOPO®TA Cloning®Kit, Dual Promoter, Invitrogen). For antibody detection, mouse monoclonal anti-acetylated α tubulin (1:250, Sigma, T6793), rabbit anti-GFP (1:1000, Torrey Pines Biolabs, TP 401), anti-HuC/HuD (1:500, Molecular Probes) and anti-BrdU (1:100, Roche) were used as primary antibodies, and Alexa Fluor 488-conjugated and 568-conjugated (1:200, Molecular Probes) secondary antibodies were used. For nuclear staining, TOTO®-3 Iodide (1:4000, Life Technologies) was used.

2.3 Morpholino antisense oligonucleotide injections

Antisense splice blocking morpholino oligonucleotides (MOs) against the *sema5a* splice donor site of exon 7 (5'-CTT CTT TAC TTA CAC ATT ACT GGT G-3') (Hilario et al., 2009) were injected in one- to four-cell zebrafish embryos at 18, 36

or 72 ng/embryo using standard procedures.

2.4 BrdU pulse labelling of habenular precursors

BrdU pulses were applied to nss$^{+/-}$ incross embryos at 32 hpf or 50 hpf as previously described (Shepard et al., 2004) with the following modifications: after BrdU uptake on ice, embryos were washed several times in warm E3 medium and let develop in the dark until 5 dpf. Treated larvae were then fixed in sweet PFA (4% PFA, 4% sucrose in 1xPBS) and brains were dissected by removing the epidermis using forceps (Turner et al., 2014).

2.5 Lipophilic dye retrograde labelling of habenular efferent axons

Larvae were fixed at 5 dpf by overnight incubation in sweet PFA and brains were dissected as previously described (Turner et al., 2014). The larvae were then pinned to a sylgard coated petri dish in 1xPBS and the fluorescent carbocyanine dyes 1,1'-dioctadecyl-3,3,3',3'-tetramethylindocarbocyanine perchlorate (DiI) and 3,3'-dioctadecyloxacarbocyanine perchlorate (DiO) (Molecular probes) were applied to the right and left exposed habenular nuclei, respectively, using tungsten needles that were tipped with dye crystals and connected to a micromanipulator. Larvae were then incubated in 1xPBS overnight at 4°C and axonal labelling was visualised by laser scanning confocal microscopy (Leica TCS SPE).

2.6 Wnt agonist/antagonist pharmacological treatments

Dechorionated embryos of a nss$^{+/-}$;Tg(pku558:GFP) incross were incubated from 32-48 hpf at 28.5°C in the dark, rocking, in either the Wnt signalling antagonist IWR-1 (50 μM, 1%DMSO, 0.002% PTU in E3; Sigma), the Wnt signalling

agonist BIO (5 μM, 2% DMSO, 0.002% PTU in E3; Sigma) or control solution (1% DMSO, 0.002% PTU in E3). Embryos were then extensively washed in fish water, let develop in fish water with 0.002% PTU until 4 dpf and fixed for immunolabelling.

2.7 Axotomies

Dechorionated Tg(lhx2a:gap-YFP) embryos at 48 hpf were anesthetised with Tricane (0.02%, Sigma) and serially mounted dorsally in a gridded petri dish lid using a 1% low-melting point agarose, 0.02% Tricane and 0.002% PTU in fish water solution, and submerged in Fish water.

To perform the ablation of lhx2a^{tg+} neurons, mounted embryos were placed in a confocal laser scanning microscope (Leica TCS SP8) coupled with a multi-photon system (Chameleon Compact OPO-Vis, Coherent) using a 25x/0.95 N.A. water objective. The region in the axonal tract to be ablated on the left or right side was first visualized using the Argon laser and targeted using the Bleach Point function in the Leica software. To ablate the axons, the multi-photon laser was tuned to 910 nm and 1 or 2 pulses with an output power ±80mW were delivered for 1.75 s each. Embryos were then carefully removed from the agarose, let develop until 72 hpf in fish water with 0.002% PTU and fixed.

2.8 Quantification of parapineal projections and BrdU pulse labelled nuclei

The parapineal projections' Z-stacks were singled-out by cropping using the Volocity software (PerkinElmer) and resliced in the X-axis with 1 μm spacing using ImageJ. The total area of each stack was then measured using the Measure tool in ImageJ and the centre of the parapineal was manually set as the origin in each image.

BrdU pulse-labelled nuclei were semi-automatically counted using an ImageJ macro specifically written for the purpose. (Suplemmentary Material A.1).

2.9 Microscopy and image manipulation

Fluorescent labelling was imaged by laser-scanning confocal microscopy (Leica TCS SP8) using 25x, 63x water or 40x oil objective lenses and z-stacks were typically acquired at 1-2 μm intervals. Images were processed using Volocity (PerkinElmer) for 3D projections and/or using imageJ (Rasband, 1997) and image manipulation for publication was performed using Powerpoint (Microsoft).

For the high quality images required for the semi-automatic counting of nuclei in BrdU pulse-labelled embryos, a 40x/1.30 N.A. oil objective was used, and images were acquired with a minimum of 1 μm z-stack interval and 1024 x 1024 pixel resolution.

Time lapse recordings of lhx2a:gap-YFP^{Tg+} axotomised embryos were imaged using the Argon laser and a 25x/0.95 N.A. water objective with incubation at 28^{o}C. Z-stacks were captured with a 2 μm spacing and 15 minutes time interval.

2.10 Statistics

All statistical operations and plot design were performed using STATISTICA (StatSoft) and Prism 6 (GraphPad), respectively. A Student t-test was used to compare habenular sizes and a multi-factorial ANOVA with a Tuckey HSD post-hoc test was used to compare the counted nuclei in the BrdU pulse experiments.

Chapter 3

Results

3.1 dHbL axons fail to correctly innervate the dIPN in *nss* mutants

As previously mentioned, the dHbL mainly projects to the dIPN while the dHbM primarily innervates the vIPN in the zebrafish midbrain. Since in *nss* mutants the dHbL is enlarged in both left and right sides, with dHbM being concomitantly reduced, it would be expected that the majority of axons from left and right habenula nuclei would converge to the dIPN. Surprisingly, retrograde lipophilic dye labelling revealed that in *nss* mutants both dHbM and dHbL neurons mainly project their axons to the vIPN (Figure 3.1C-C'), while wild-type siblings display a normal pattern of IPN innervation (Figure 3.1D-D'). Additionally, Pku558^{+} neurons, which are still asymmetrically specified on the dHbL of *nss* mutants, also preferentially, but not exclusively, innervate the vIPN (Figure 3.1E-E'). With both techniques we could also assess that these neurons extend their axons more posteriorly, suggesting that the innervation to the raphe nuclei remains unaffected (Figure 3.1C-D,E-F, white asterisks). Taken together, these results indicate that, although left and right habenula acquire left-type phenotype, right and left dHbL neurons fail to project to the dIPN. In fact, some axonal tracts from both sides seemingly miss the IPN altogether, continuing to advance ipsilaterally to more posterior regions (Figure 3.1D, white arrow heads). In addition, a closer inspection of the IPN in *nss* mutants shows an apparent L-R segregation between

axons arriving from both habenulae, frequently displaying a gap in the region of the midline (Figure 3.1D), which is suggestive of midline defects in this mutant background.

Indeed, an intact midline is required for early asymmetric markers to be correctly expressed in only one side of the brain (Concha et al., 2000). To assess whether the IPN phenotype observed in *nss* mutants could be partly due to midline defects, we probed for the expression of the floor plate and notochord marker *sonic hedgehog* (*shh*). At 24 hpf we could not detect any differences in the expression domain of *shh* in wild-type siblings (Figure 3.2A-A') and nss$^{-/-}$ (Figure 3.2B-B'), suggesting that there are no major defects in midline tissues development in these mutants.

Additionally, guidance cues such as Slits, Ephrins and Semaphorins are required to repel commissural axons to the contralateral side once they have reached the floor plate (Nawabi and Castellani, 2011). To address if commissural axons are being correctly guided through the midline in *nss* mutants, we have analysed the formation of the post-optic commissure (POC) and anterior commissure (AC) in the forebrain by acetylated α-tubulin staining at 28 hpf embryos. Although most POC and AC axons correctly crossed the midline in all wild-type siblings examined (Figure 3.2C), 6/10 *nss* mutant embryos displayed abnormal crossing of commissural axons, particularly in the AC (Figure 3.2D, white arrow heads), suggesting that midline-derived axonal guidance cues are disrupted in *nss* mutants.

Previous studies have demonstrated that the secreted Class III Semaphorin, Sema3D, and its Neuropilin family receptor, Nrp1a, act as guidance cues to direct dHbL axons to the dIPN (Kuan et al., 2007). Indeed, *nrp1a* was shown to be specifically expressed in the left habenula as early as 2 dpf, while *sema3D* is expressed in the midline between the dHb and the IPN at this timepoint. Also, Nrp1a and/or Sema3D depletion by morpholino (MO) injection leads to the majority of *kctd12.1*$^{+}$ neurons to project to the vIPN. It is thus possible that the failure of dHbL axons to project to the dIPN in *nss* mutants is caused by defective guidance modulated by Nrp1a/Sema3D signalling. To test this hypothesis, we checked *nss* mutants for the expression of *nrp1a*. As previously reported, *nrp1a* is specifically expressed in the left habenula in wild-type siblings at 4 dpf (Figure

3.1A). In *nss* mutants, however, this expression is greatly reduced (Figure 3.1B).

Taken together, these results indicate that the failure to correctly express *nrp1a* in the dHbL and, consequently, to respond to Sema3D signalling in *nss* mutants might preclude dHbL axons from properly projecting to the dIPN, thereby converging with dHbM axons in the vIPN. Additionally, failure in Sema3D-mediated midline signalling might explain the observed L-R segregation of habenular axons in the IPN of *nss* mutants.

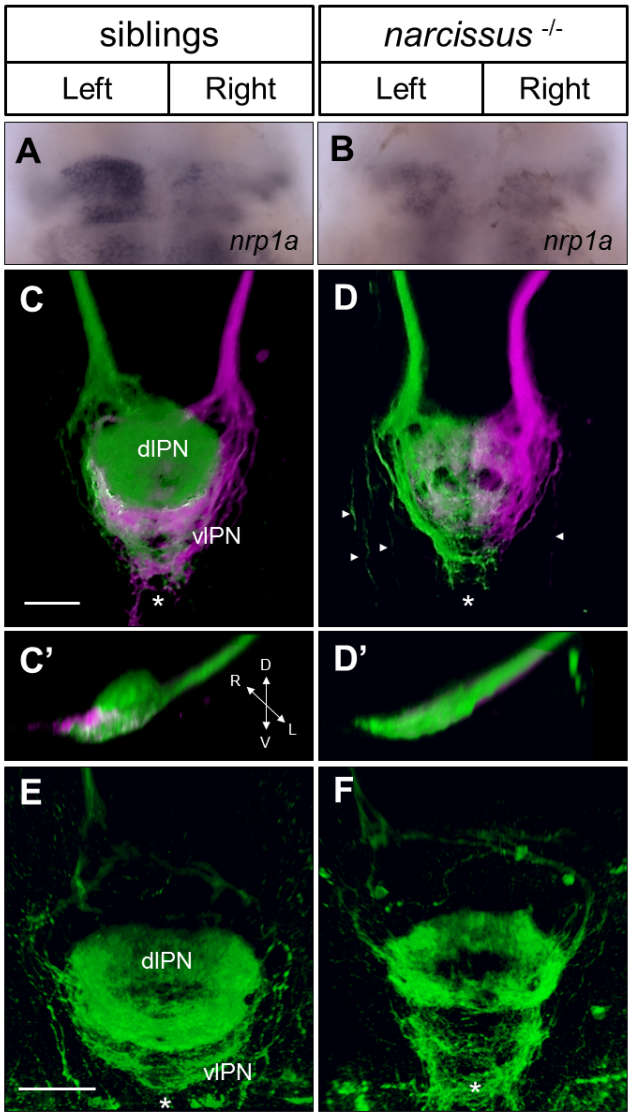

Figure 3.1: **dHbL axons innervation pattern is affected in *nss* mutants.** **A,** *In situ* hybridization of *nrp1a* in wild-type siblings and **B,** *nss* mutants. **C,C',** Retrograte dye labelling reveals that left habenular (lHb) axons (green) mainly project to the dorsal interpeduncular nucleus (dIPN) while right habenular (rHb) axons (magenta) innervate almost exclusively the ventral interpeduncular nucleus (vIPN) in 4dpf wild-type siblings, but **D,D'** both lHb and rHb axons converge to the vIPN in 4dpf *nss* mutants. lHb and rHb nuclei were labelled with DiO and DiI, respectively. **E,** Immunolabelling of Tg(Pku558:GFP) neurons reveal that these project to the dorsal IPN in wild-type siblings, while in *nss* mutants **F,** the pattern of projection is affected, with pku558^{+} neurons projecting mostly to the vIPN. White arrowheads indicate misdirected axons projecting posteriorly. White asterisks represent the raphae nuclei. Scale bars = 25 μm. Anterior is to top in C,D,E and F and to the right in C' and D'.

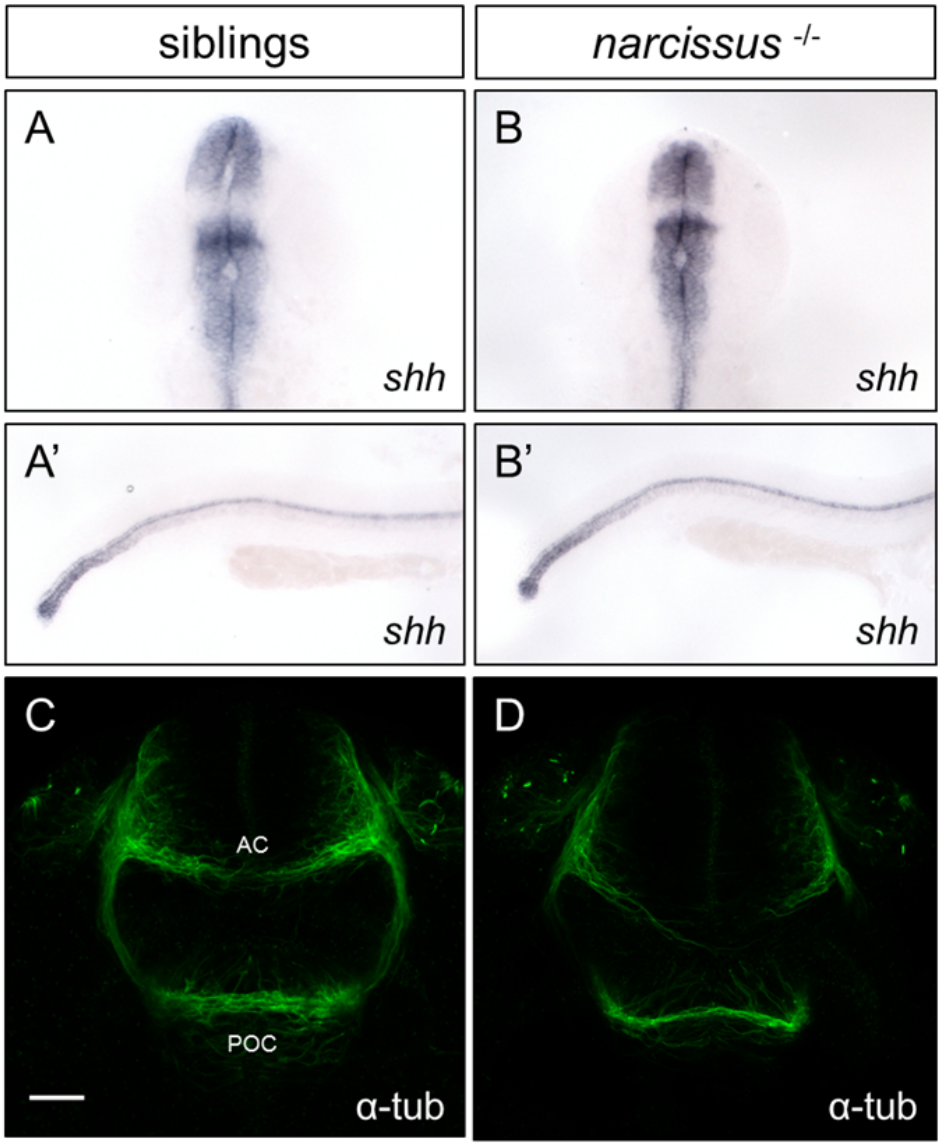

Figure 3.2: ***nss* mutants have normal midline tissues development but display defects in commissure formation.** **A-B',** *sonic hedgehog* (*shh*) is correctly expressed in the floorplate and notochord in both wild-type siblings, **A-A'** and *nss* mutants **B-B'** at 24 hpf. **C-D,** acetylated α-tubulin immunostaining of the anterior commissure (AC) and post-optic commissure (POC) at 28 hpf reveals that **C,** they are normally formed in wild-type siblings (n = 12) but **D,** AC axons fail to cross the midline in 6/10 analysed *nss* mutants. Scale bar = 25 μm. Anterior is to the top in A and B and to the right in A' and B', while dorsal is to the top in C and D.

3.2 Parapineal and olfactory bulb efferent projections to the habenulae are affected in *nss* mutants, and projections from the pallium remain asymmetric

The parapineal axonal projections to the left habenula have a critical role in the acquisition of dHbL fate, as specific ablation of parapineal anlage prior to its leftward migration or inhibition of the latter leads both habenulae to acquire a right-sided fate (Gamse et al., 2003). Considering this, it is possible that the left-type isomerism observed in *nss* habenular nuclei might be a result of defective parapineal-mediated induction of habenular fate.

We have previously observed that the parapineal organ correctly migrates to the left side in *nss* mutants (Figure 1.5A-B). To clearly visualize axonal trajectory of parapineal neurons and to assess whether the pattern of innervation is affected in mutants, we have carefully analysed axonal processes in confocal optical sections of 4dpf Tg(foxD3:GFP) embryos. We found that, unlike in wild-type sibling (Figure 3.3A) where axonal terminations tend to accumulate closer to the parapineal, these seem to extend onto a broader region of the left habenula in $nss^{-/-}$ (Figure 3.3B). In addition, we observed some axonal projections directing toward the midline in mutants. These observations were further confirmed by quantification of the total area of projections in relation to their distance to the parapineal (Figure 3.3E).

More recently, Miyasaka and colleagues have described another asymmetric afferent projection specific to the right habenula, originating from a population of mitral cells in the zebrafish olfactory bulb (OB) and labelled by gap-YFP expression in Tg(lhx2a:gap-YFP) embryos (Miyasaka et al., 2009). Analysis of Tg(lhx2a:gap-YFP) embryos revealed that $lhx2a^{tg+}$ neurons fail to extend neuronal processes to the right habenula nucleus in *nss* mutants at 5 dpf (Figure 3.3D-D'), in contrast to wild-type siblings and consistent with the bilateral left-sided identity of habenular neurons (Figure 3.3C-C').

Cells labelled by transgenic expression in Tg(ClnB:GFP), probably originating in the pallium, were identified by our lab to specifically project to the left

habenula. If the left-sided isomerism observed in the habenulae of *nss* mutants is complete, we would expect to see these neurons projecting to the rHb as well as to the lHb. An analysis of these projections in *nss* mutants, however, revealed that ClnB^{Tg+} neurons still project asymmetrically to the left habenula (Figure 3.3E-F').

Taken together, these results show that in *nss* mutants there is an overall disruption in habenular afferent projections, non-concordantly with a complete bilateral specification of the habenulae.

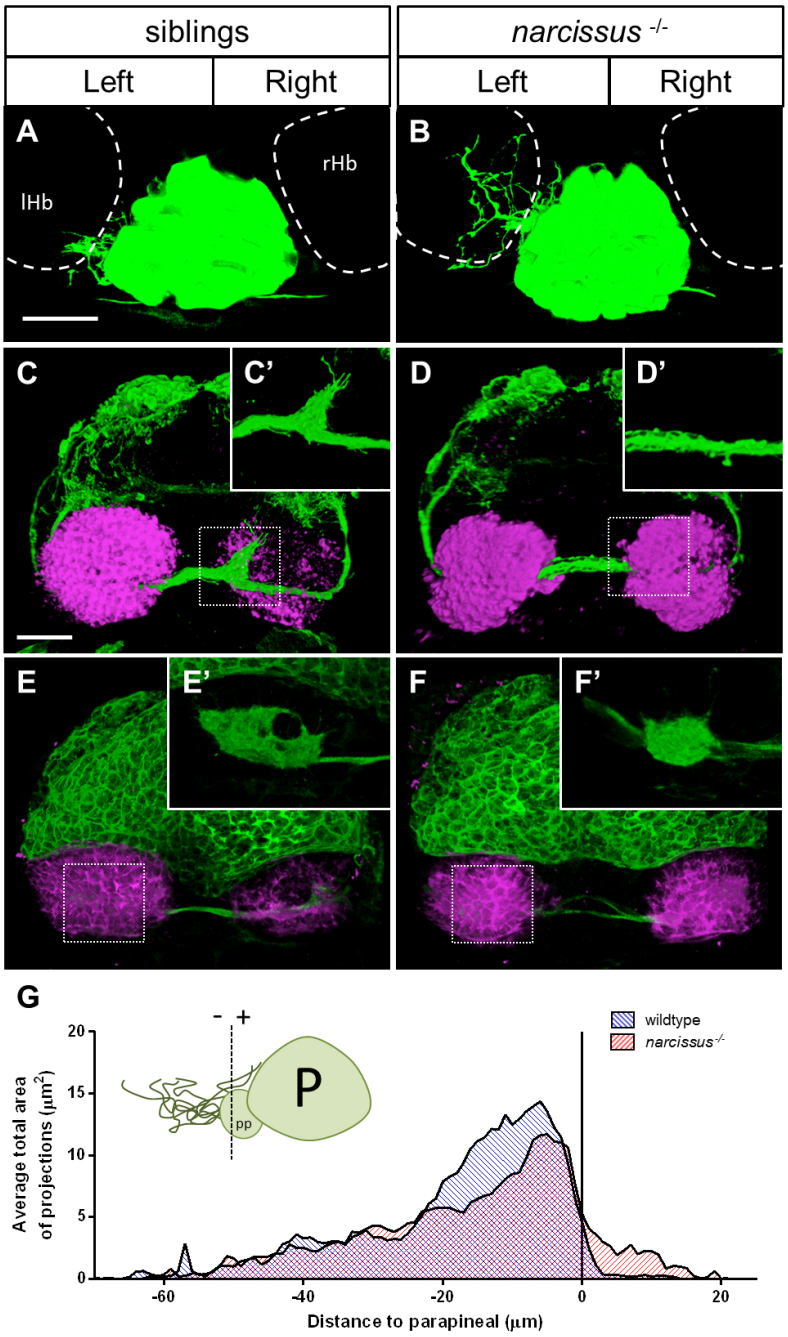

Figure 3.3: **Asymmetric afferent projections to the dHb are disrupted in *nss* mutants. A-B,** Immunolabelling in of Tg(foxD3:GFP) at 4 dpf reveals that the parapineal (pp) innervation to the left habenula nucleus (lHb) extends towards a broader region in *nss* mutants **(B)** than in wild-type siblings **(A)**. **C-D',** Immunolabelling of lhx2a^{tg+} (green) olfactory bulb asymmetric projections to the right habenula (rHb) coupled with fluorescent *in situ* hybridization of *kctd12.1* (magenta) shows that these are completely absent in *nss* mutants at 5 dpf.

Figure 3.3: **E-F',** Immunolabelling of ClnB^{tg+} (green) pallium asymmetric projections to the left habenula (lHb) coupled with fluorescent *in situ* hybridization of *kctd12.1* (magenta) shows that these remain asymmetric in *nss* mutants. **G,** Quantification of the parapineal projections pattern by correlation of the average area of the projections with the distance to the parapineal (n = 19). Positive values represent distances to the left while negative values represent distances to the right of the parapineal. White dotted boxes represent the zoomed region in C',D',E' and F'. Scale bar = 25 μm. P, pineal.

3.3 Axonal projections in Tg(lhx2a:gap-YFP) are not required for dHbM fate induction

As *kctd12.1* bilateral expression in *nss* mutant habenulae only develops from 48 to 72 hpf onwards, and no asymmetric disruption is seen before 48 hpf, we have hypothesised that what mediates this disruption might act during or from that time period onwards. We performed a time-course analysis revealing that the asymmetrical projection of lhx2a^{tg+} OB neurons into the right habenula nucleus is first apparent at 52 hpf (Supplementary Figure B.1C, white arrowhead). The complete lack of these efferent projections in *nss* mutants, together with the fact that these innervate the right habenula nucleus at a seemingly critical time period in the development of the asymmetric defects observed in this mutant background led us to hypothesise that asymmetrical epithalamic innervation by OB mitral cells play a role in the development of right habenula identity. Much like what has been described for the inductive role of the parapineal in lHb development, mitral cells innervation to the right habenula progenitors could directly or indirectly promote dHbM or repress dHbL fates in this nucleus. As such, a failure to innervate the rHb in *nss* mutants would account for the failure to induce a right-type phenotype in the right epithalamus. To test this hypothesis, we conducted a laser-mediated axotomy of the axonal fibre bundles in Tg(lhx2a:gap-YFP). Using a multi-photon laser coupled with a confocal microscope, both left and right fibre bundles were selectively severed at around 48 hpf, before they had reached the epithalamic region. After the axotomy, embryos were left to develop until 72 hpf and then labelled for both the transgenic and either *kctd8* or *kctd12.1*

expression as markers of dHbM and dHbL fates, respectively. Control embryos were subjected to the same laser pulses but in a YFP negative region close to the fibre bundles (Figure 3.4A-H). Time-lapse analysis after the axotomies and immunodetection of YFP in fixed embryos revealed that, unlike expected, the severed axons did not grow back, but rather regressed to their cell bodies in the OB (Supplementary Figure B.2). Despite this, *kctd8* and *kctd12.1* asymmetric expression domains were comparable in both axotomised and control embryos at 72 hpf (Figure 3.4A-H). These results indicate that, although present at the correct timing, OB mitral cells asymmetrical projections to the right habenula are not required to promote dHbM fates in the right epithalamus, and so, the observed lack of these projections in *nss* mutants are most likely a consequence and not a cause of the bilateral left-sided character in the habenulae of these mutants.

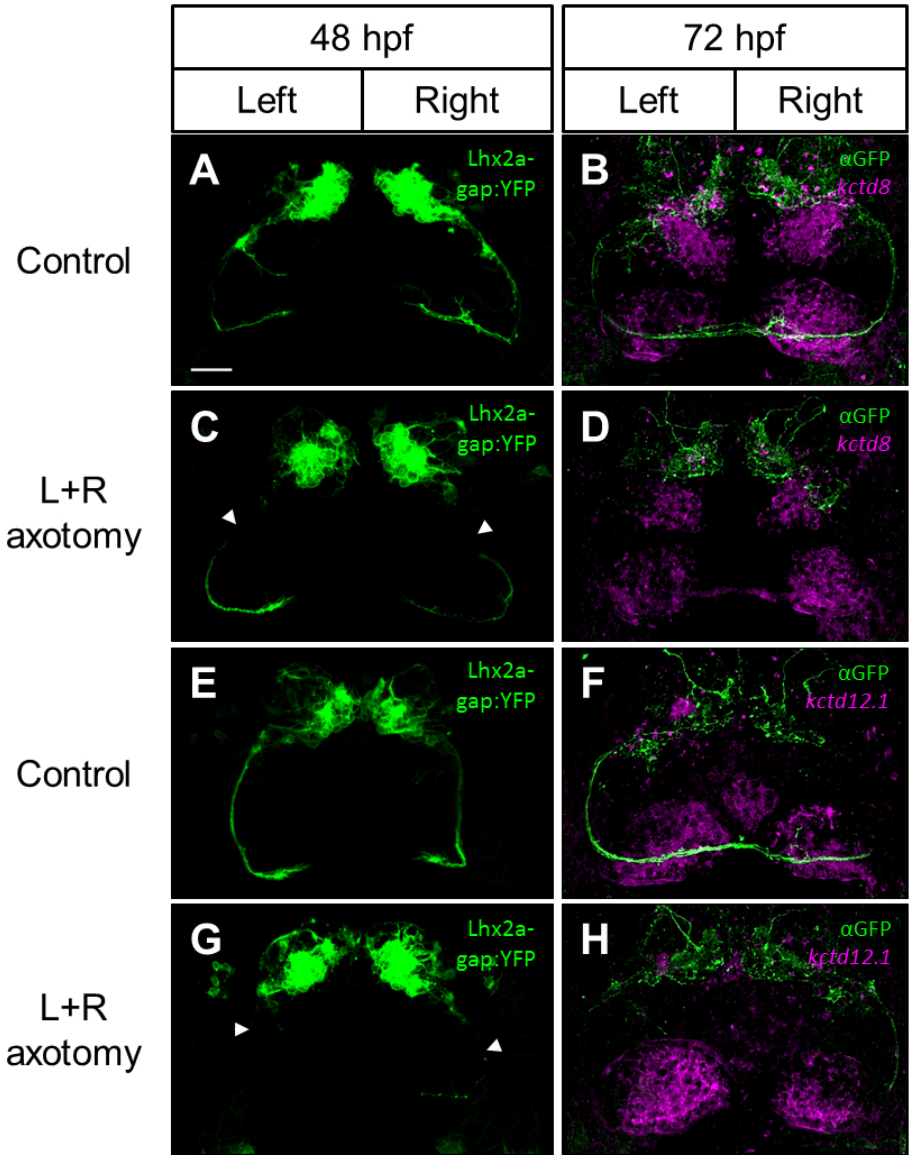

Figure 3.4: **Asymmetric afferent projections from the OB in Tg(lhx2a:gap-YFP) are not required to specify dHbM neurons. A,E,** Left and right lhx2a^{Tg+} lateral fasciculi axotomised and **C,G,** non-axotomised controls display normal expression of both the **B,D,** dHbM marker *kctd8* and **F,H,** dHbL marker *kctd12.1*. Images in A, C, E and G represent the endogenous *in vivo* transgenic expression of Tg(lhx2a:gap-YFP) after the administration of the laser pulses at 48hpf, while embryos in B,D,F and H represent these same embryos fixed at 72 hpf, immunolabelled against GFP (green) and probed for either *kctd8* or *kctd12.1* expression by fluorescent *in situ* hybridization (magenta). Arrowheads in C and G indicate where the axotomy pulses were administred. Scale bar = 25 μm.

3.4 Habenular neurogenesis is affected in *nss* mutants

One of the mechanisms through which is possible to explain the development of an asymmetric habenula is the asymmetric onset of neurogenesis in left versus right epithalamus. dHbL and dHbM neurons are born at different time points during development: while the majority of dHbL neurons are born at around 32 hpf on the left habenula, most dHbM neurons are specified around 50 hpf on the right habenula (Aizawa et al., 2007). One possible explanation for the double left-sided phenotype in *nss* mutants is a disturbance in the asymmetric onset of neurogenesis, leading to both left and right dHb neurons being born during the first wave of neurogenesis and thereby acquiring a dHbL fate. Another explanation is that both left and right-sided neurons are correctly born during the first and second neurogenic waves, respectively, but a failure to induce dHbM character in neurons born during the second wave would result in the ectopic specification of a dHbL fate. To distinguish between these two hypotheses and to identify when ectopic right-sided *kctd12.1*$^{+}$ neurons are born in *nss* mutants, we conducted a birth-date analysis of habenular neurons by BrdU pulse labelling at both 32 hpf and 50 hpf (Figure 3.5C-F,J). After BrdU pulse, embryos were chased until 5 dpf, a time point where both asymmetric gene expression and laterotopic projections are already established, and probed for *kctd12.1* expression to mark dHbL (*kctd12.1*$^{+}$) and dHbM (*kctd12.2*$^{-}$) domains.

In both *nss* mutants and wild-type siblings, BrdU cells labelled at 32 hpf acquired a more dorsal and lateral position in the both habenulae, while cells labelled at 50 hpf typically acquired a ventral and medial position (Figure 3.5C,E), as previously described (Aizawa et al., 2007). In respect to their L-R disposition, no significant differences in the number of proliferating (BrdU^{+}) cells were found between left and right habenular nuclei in wild-type siblings when the pulse was administered at 32 hpf, though significantly more of these cells acquired a dHbL fate (*kctd12.1*$^{+}$) on the left side compared to the right (Figure 3.5C,G,J). In contrast, no L-R differences in either the total number of BrdU^{+} or *kctd12.1*$^{+}$ cells were found in *nss* mutants at this timepoint (Figure 3.5D,H,J). BrdU pulse at 50 hpf revealed that, as expected for this time point, significantly more cells

proliferate on the right habenula of wild-type siblings (Figure 3.5E,J), although no significant L-R differences were detected in total BrdU incorporation in *nss* mutants (Figure 3.5F,J). Furthermore, no significant asymmetries were found in BrdU$^+$ and *kctd12.1*$^+$ cells for either genotype (Figure 3.5E,F,J). Surprisingly, *nss* mutants have significantly less BrdU labelled cells than wild-type siblings in both left and right habenulae at 32 hpf and on the right habenula at 50 hpf (32 hpf: sibsL = 151.5±27.5, nssL = 114.8±25.5, P<0.005; sibsR = 145.3±23.9, nssR = 108.9±34.8, P<0.005; 50 hpf: sibsL = 82.8±24.7, nssL = 70.3±17.2, P>0.05; sibsR = 109.4±27.3, nssR = 72.9±19.8, P<0.0001; n = 15 for each genotype and timepoint). This reduced labelling also seems to have a bigger impact on dHbL neurons on the left side and dHbM neurons on the right side: significantly less *kctd12.1*$^+$, but not *kctd12.1*$^-$, cells are found in the lHb of 32 hpf BrdU labelled embryos, while significantly less *kctd12.1*$^-$, but not *kctd12.1*$^+$, cells are found in the rHb of both labelled timepoints. In fact, there appears to be a small, though non-significant, increase in *kctd12.1*$^+$ cells on the rHb of *nss* mutants compared to wild-type siblings in both timepoints (Figure 3.5J).

The reduced number in BrdU positive (for both time points) and *kctd12.1*$^+$ cells in *nss* lead us to question whether *nss* mutants have decreased habenulae size altogether. To test this, we measured the area of both habenulae using a z-stack projection of the nuclei marker to infer the limits of the habenula structure. Since the degree of nuclear compaction does not differ between wild-type and mutants, the measurement of habenula nuclei area is a good estimation for total number of cells. As expected, *nss* mutants show statistically significant smaller habenulae on both sides (±15%) (Figure 3.5G-I).

Taken the above results in consideration, it is also possible that despite their birth date, neurons in the rHb are being specified early in the same timepoint as lHb neurons, thus acquiring a dHbL fate. To check if asymmetric specification of neurons is still present in *nss* mutants, we analysed the number of cells that express the early neurogenic marker HuC/HuD between left and right habenulae at 36hpf (Figure 3.5A-B). Similarly to previous accounts (Roussigné et al., 2009), HuC/HcD was expressed asymmetrically in the left habenula in both wild-type siblings and *nss* mutants, and no significant difference was also found between the asymmetry quotients of both genotypes (L/(L+R): sibs = 0.670±10.2, nss =

0.674±0.2; P>0.95; n=16), indicating that the onset of asymmetric neurogenesis is not affected in *nss* mutants. This is also further supported by the conservation of a larger left habenular nucleus in *nss* mutants.

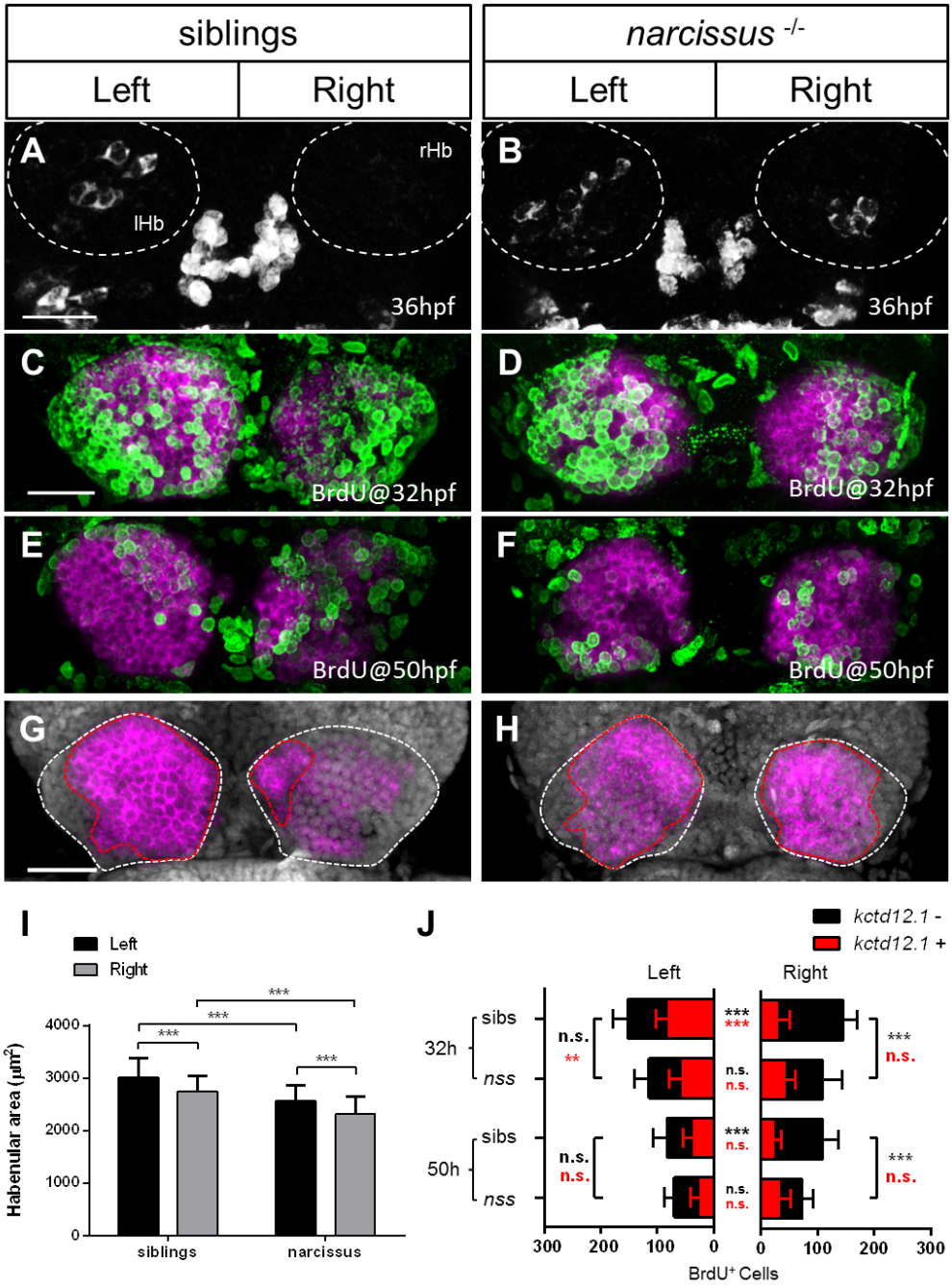

Figure 3.5: **Habenular neurogenesis is affected in *nss* mutants. A-B,** HuC/HuD immunolabelling of new-born neurons at 36 hpf in **A,** wild-type siblings and **B,** *nss* mutants. **C-D,** Habenulae of 5 dpf BrdU pulse-labelled embryos at 32 hpf or **E-F,** 50 hpf (green) and probed for *kctd12.1* expression (magenta). **G-H,** z-stack maximum projections of 5dpf embryos stained for nuclear (grey) and *kctd12.1* (magenta) expression. **I,** Quantification of the left and right area of the habenular nuclei in wild-type siblings and *nss* mutants (n=15 for each genotype).

Figure 3.5: **J,** Quantification of BrdU pulse-labelled cells in wild-type siblings and *nss* mutants at both 32 and 50 hpf. Significance values in the middle represent differences between sides in either *kctd12.1*$^{+}$ (red) or *kctd12.1*$^{-}$ (black) domains. Significance values in the margins represent differences on the same side between genotypes. Dotted white lines in A, B, G, and H represent the habenular nuclei and dotted red lines in G and H demark the *kctd12.1* expression domain. Scale bars=25 μm. lHb, left habenula; rHb, right habenula; n.s., non-signifficant; ** P <0.005; *** P <0.0001.

3.5 Wnt signalling acts upstream or independently of *nss* to determine habenular neuronal fate

It has been proposed that Wnt/β-catenin signalling modulates the asymmetric fate of dHb neurons by inducing them to acquire a dHbM character, and that the parapineal might function to inhibit Wnt signalling on the lHb, thereby allowing neurons on that side to acquire a dHbL fate (Hüsken U. and Carl M.; personal communication). Considering this, it is possible that in *nss* mutants, an untimely inhibition of Wnt signalling in the rHb is able to account for the bilateral left-sided character observed. To test if Wnt signalling is affected in *nss* mutants, Tg(Pku558:GFP) embryos were treated with either IWR-1, a small molecule that inhibits Wnt/β-catenin response by stabilizing Axin proteins (Chen et al., 2009), BIO, an agonist of Wnt/β-catenin signalling that functions by inhibiting GSK-3 (Meijer et al., 2003), or 1% DMSO as control. Embryos were treated from 32-48 hpf and let develop until 4 dpf, where they were fixed and immunolabelled for the transgenic expression and acetylated α-tubulin for neuropil and habenula commissure labelling (Figure 3.6A-F).

As previously described (Hüsken U. and Carl M.; personal communication), all IWR-1 treated embryos showed an increase in Pku558 expression in the rHb. Additionally, embryos exposed to BIO treatment displayed a significant reduction in Pku558 expression in both habenulae compared to controls but no loss of asymmetry (Figure 3.6A,C,E). Likewise, *nss* mutants showed the same effect as

wild-type siblings in both treatment conditions (Figure 3.6B,D,F). To confirm the efficiency of the drugs in disrupting Wnt signalling, Tg(7Xtcf-siam:GFP)^{ia4} embryos, a transgenic reporter of the pathway in the lateral line, were exposed to the same treatments as *nss* mutants and wild-type siblings. As previously reported, BIO treatment led to an early arrest in the migration of lateral line primordium (Valdivia et al., 2011), yet no apparent phenotype was observed in either IWR-1 or control treated embryos (Supplementary Figure B.3).

IWR-1 and BIO treatments additionally led to gross defects in the habenular commissure, as evidenced by acetylated α-tubulin staining. IWR-1 treated embryos frequently displayed additional and erratic wiring of the two habenulae, sometimes even extending to the telencephalon (Figure 3.6C,D), while BIO treated embryos showed the opposite effect, with a severe reduction in both the habenular commissure wiring and habenular neuropil (Figure 3.6E,F).

Together, these results indicate that Wnt signalling acts in the habenulae to promote dHbM fate and habenular commissure formation, but is not likely disrupted in *nss* mutants, possibly acting either upstream or independently of the mutation.

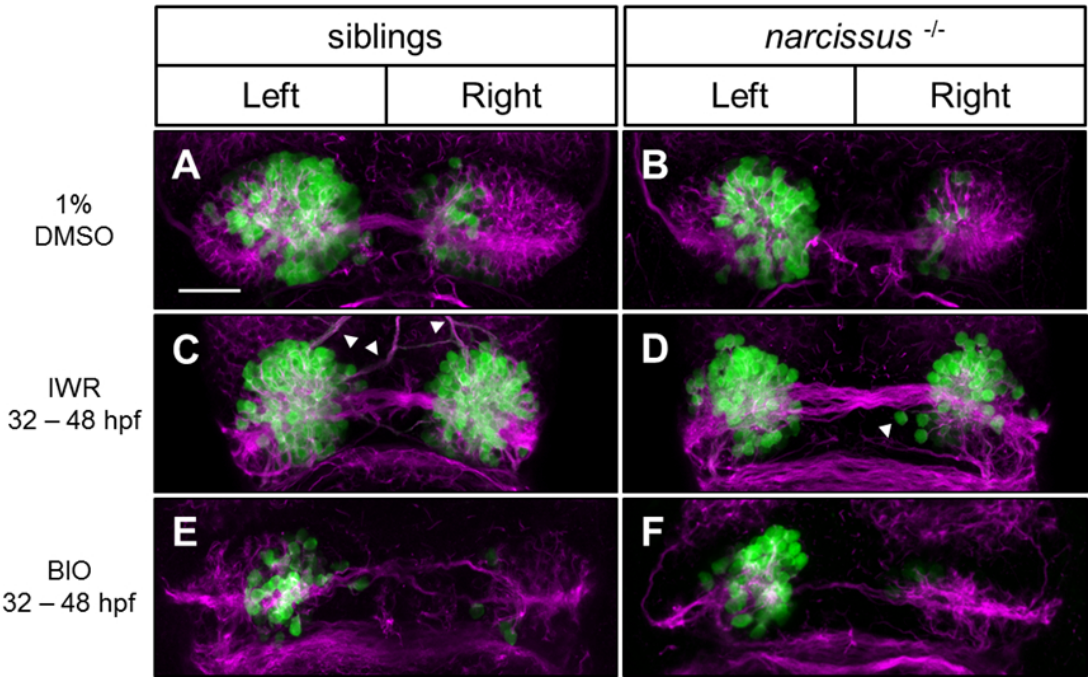

Figure 3.6: **Modulation of canonical Wnt signalling through pharmacological treatments alters habenular development in both wild-types and *nss* mutants. A-F,** Wild-type sibling and *nss* mutant embryos treated from 32–48 hpf with **A-B,** 1% DMSO control, **C-D,** IWR-1 mediated Wnt signalling inhibition or **E-F,** BIO mediated Wnt signalling hyperactivation. Embryos were fixed at 4dpf and immunolabelled for transgenic expression of Pku558:GFP (green) and acetylated α-tubulin (magenta). Arrowheads indicate habenular commissure errant axons. Scale bar=25 μm.

Chapter 4

Discussion

In this study we described a novel mutant, *narcissus* (*nss*), which displays defects in diencephalic L-R asymmetries. *nss* mutants are characterized by the bilateral expression of the left-sided dominant dHbL marker *kctd12.1*. Contrary to what has been previously described, and despite displaying a dHbL molecular signature, both left and right habenula neurons of *nss* project to the ventral IPN, instead of the dorsal IPN, the preferential target of dHbL neurons (Aizawa et al., 2005). Interestingly, the same IPN phenotype is observed in embryos where the left habenula marker *nrp1a* and/or its midline expressed ligand *sema3D* are knockdown. As *nrp1a* expression is absent in the lHb of *nss* mutants, it is possible that the defects in habenular neurons innervation patterns axons observed in these mutants are a consequence of a deficient Nrp1a/Sema3D-mediated attractive signalling to the dIPN. Noteworthy, a vIPN preferential convergence of habenular axons was also reported in *sec61al1* mutants, who also display a left-type isomerism phenotype in the habenulae, but *nrp1a* is bilaterally expressed (Doll et al., 2011). Although other phenotypes in *sec61al1* are dissimilar to the ones observed in *nss* mutants (see below), and the authors do not advance any explanation for this contradicting IPN phenotype, it is possible that the mechanisms behind the two are similar.

Unlike previously reported left-sided dHb isomerisms, *kctd12.1* expression still develops asymmetrically at 2 dpf in *nss* mutants, only becoming bilateral from 3 dpf onwards. This could lead us to assume that *nss* might act during this period to establish asymmetric specification of dHb neurons to the dHbL subtype

fate. Consistent with this, the earliest neurons to be asymmetrically specified to the dHbL and labelled by transgenic expression in Tg(Pku558:GFP) embryos (Hüsken U. and Carl M.; personal communication) are still asymmetrically expressed in the lHb in *nss* mutants. How can we explain this apparently incomplete disruption of asymmetry in the dHb of *nss* mutants? Several events occur during this critical period of time in the zebrafish epithalamus. The parapineal starts its leftward migration from the pineal stalk at around 28 hpf and starts projecting to the lHb at 48 hpf (Concha et al., 2003). Failure to migrate or specific ablation of parapineal cells prior to migration leads the majority of neurons in the lHb to acquire dHbM character, thus leading to the hypothesis that the parapineal is crucial for dHbL neuronal specification (Gamse et al., 2003). Our results show that in *nss* mutants the parapineal correctly migrates to the left and projects to the lHb, consistent with correct dHbL neuronal specification on that side. Interestingly, the parapineal axonal projections seem to extend more widely in mutants, but also with some axonal terminations being formed towards the midline. This might lead us to hypothesise that a parapineal axon-mediated signal could be responsible to induce dHbL specification on the rHb of *nss* mutants. This however seems unlikely, as no parapineal projections were ever observed reaching the rHb, thus indicating that their disruptive innervation pattern is more likely to be a consequence than a cause of the phenotype. Several lines of evidence also suggest that the parapineal might act to inhibit dHbM fate on the lHb by repressing Wnt signalling on that side in a Tcf7l2-dependent manner. Indeed, *tcf7l2* mutants display dHb left-sided isomerism in respect to gene expression and efferent connectivity, even upon parapineal ablation (Hüsken U. and Carl M.; personal communication). In *nss* mutants, however, inhibition of the pathway from 32-48 hpf by pharmacological treatments led to a complete double left-sided expression of Pku558:GFP in all embryos, suggesting that a downregulation of Wnt in the rHb is not likely to account for the bilateral expression *kctd12.1* in these mutants. Despite this, it is still possible that a downregulation of Wnt after 48 hpf would only impact on *kctd12.1*$^+$ neurons and not on Pku558$^+$ ones, as the latter are specified prior to this time point. Inhibition of Wnt signalling at later timepoints and selective ablation of the parapineal coupled with *kctd12.1* probing will help resolve this issue.

Just like the parapineal has an instructive role in determining dHbL fate on the lHb, it is plausible that other asymmetrical inputs to the dHb have a similar instructive role in habenular neuronal fate specification. We have identified that the previously reported asymmetrical projection of OB mitral cells to the rHb is completely absent in *nss* mutants at 5 dpf. This projection arises from axons crossing the habenular commissure at around 52 hpf, concordant with the critical period in which bilateral *kctd12.1* expression becomes evident in *nss* mutants. It seemed thus a possibility that signals arriving from these neuronal terminations to the rHb could induce dHbM fate specification on that side, perhaps by mediating signalling pathways known to be involved in this decision, such as Notch or Wnt. In support of this, a recent study found that odour stimulation from the left, but not right, OB in adult zebrafish is able to induce asymmetric neuronal specification in the left ventricular-subventricular zone (V-SVZ) in a Notch-dependent way (Kishimoto et al., 2013). Likewise, other studies in fruit flies and mice have also found evidence for Notch signalling modulation in response to neuronal activity (Alberi et al., 2011; Lieber et al., 2011). Despite this, selective ablation of the axonal projections from Tg(lhx2a:gap-YFP) embryos to the rHb did not result in any significant misspecification of habenular neurons in either the right or left habenula nucleus. Arguably, the cells labelled in Tg(lhx2a:gap-YFP) are likely not to be the only ones in the OB projecting to the dHb, thereby the possibility exists that the selective axotomy performed does not impact all projections to the rHb. Perhaps just as likely is the possibility that, although not visibly identifiable, some projections to the rHb were already established by the time the axons were severed, thereby still enabling the start or amplification of dHbM specification signals. Nevertheless, these results argue against a dHbM fate specification by the asymmetric innervation of OB to the rHb.

Neurons in the dHb are thought to acquire different fates depending on the time during development in which they are born and asymmetric signals in the environment are then ultimately responsible for their L-R asymmetric disposition (Aizawa et al., 2007). Consistent with this, and using BrdU pulse labelling of habenular precursors at different timepoints, we've found that in wild-type siblings most dHbL (*kctd12.1*$^{+}$) neurons are born at 32 hpf on the lHb, while the majority of dHbM (*kctd12.1*$^{-}$) neurons are born in the rHb at both 32 and 50

hpf. In apparent contradiction with this, Aizawa and colleagues reportedly found dHbM neurons to be born only from 36 hpf, though in very small numbers, and to peak at around 48 hpf (Aizawa et al., 2007). This inconsistency is perhaps most likely explained by the use of different methodology to quantify the habenular nuclei and the use of different markers to determine their sub-nuclear identity. Also, and although the same labelling protocol was used, it is possible that in the experiments presented here the BrdU remained in the system for an increased period of time, thereby increasing the pulse and labelling cells dividing at later timepoints.

We hypothesised that a disruption in the birth-date of habenular neurons on the right side in *nss* mutants might lead them unable to perceive the signals required for dHbM specification, thus ultimately acquiring a dHbL fate. Intriguingly, *nss* mutants display an overall reduction of BrdU labelled cells in both habenulae and at both time points analysed. In addition, less dHbL, but not dHbM, neurons are born on the lHb in comparison to wild-type siblings, while the impact is significantly greater on dHbM neurons on the rHb, probably reflecting the relative contribution of the left and right habenulae to each neuronal fate. These results indicate that either loss of proliferation or increased apoptosis in the habenulae contribute to the dHb bilateral phenotype observed in *nss* mutants. Consistent with this, both habenulae are significantly smaller in size in mutants as compared to wild-type siblings.

As mentioned earlier, Notch signalling is thought to be required to delay neurogenesis on the rHb, leading neurons on that side to acquire dHbM fate, possibly due to differences in the environmental signalling. Indeed, disruptive asymmetric neurogenesis was associated with the double-left dHb phenotype in *sec61al1* mutants, in which a disruption of the apical-basal polarity of neuroepithelial cells in the diencephalon was thought to lead to the over-proliferation of neurons in both habenulae (Doll et al., 2011). In contrast with this, not only *nss* mutants display normal onset of asymmetric neurogenesis as compared to wild-type siblings, evidenced by the lHb dominant expression of the early neurogenic marker HuC/HuD at 36 hpf, but the BrdU pulse labelling indicates a reduced, rather than increased, proliferation. How then can we explain the overexpression of the dHbL marker on the rHb? One possibility is that a significant reduction of the

habenular progenitor pool leads to less dHbM neurons being specified in the rHb at early timepoints, thus promoting an over-representation of dHbL neurons on that side. If this is true, we can envision that a balance between the different habenular sub-nuclei might occur, so that if, at any given time, one is dominant over the other, the latter ends up being repressed. On the other side, increased cell death on both habenulae might lead to the same outcome. Although this is highly speculative, when Notch signalling is constitutively hyperactivated in both habenulae at 28, 32 or 36 hpf, thus hypothetically inhibiting habenular neural stem cells to undergo neurogenesis and acquiring dHbL character, an expansion of dHbM cells, labelled by *kctd12.2* expression, is observed on both sides at 56 hpf (Aizawa et al., 2007). The authors attribute this to the ability of cells to bypass the default dHbL program after Notch activation, though more evidence is required to support this hypothesis. These results might also help explain why *nrp1a* is not expressed in the lHb of *nss* mutants, as this neuronal subpopulation might be compromised by the overall reduction of habenular neurons.

The results gathered so far and the lack of identity of the mutated gene in *nss* mutants only allows us to speculate on the mechanisms by which they acquire their epithalamic phenotype. Previous work done by our lab using recombinant mapping was able to identify the putative mutation to be inserted in a 3.2Mb region (15.2-18.4 Mb) in the linkage group 24. Further analysis was however difficult as this region is close to the centromere, an area known to encompass low rates of meiotic recombination. To tackle this, DNA samples from *nss* mutants were sent for whole-genome sequencing in an attempt to pinpoint the exact location and identity of the mutation, but complications in the purification of the samples delayed the results beyond the time of submission of this thesis. Despite this, we searched the literature and gene expression databases in an attempt to reduce the number of candidate genes from those present in the region of interest (around 40). One promising candidate is *sema5a*, which encodes for the Class V transmembrane Semaphorin 5a protein. Like other Semaphorins, Sema5a is involved in axonal guidance in vertebrates and seems to be particularly required for the correct guidance of the developing axons of the *fasciculus retroflexus* that connect the habenulae to the IPN in rats (Kantor et al., 2004). Given the non-concordant mis-segregation of axons in the IPN of *nss* mutants, we hypothesised

that Sema5a could have a similar role in zebrafish, perhaps also being required for proper specification of L-R habenular asymmetries. The only study in fish so far, demonstrated by morpholino (MO) knockdown that Sema5a acts both as an attractive and repulsive cue to correctly guide motor axons in the ventral myotome, but no effects in the brain were reported (Hilario et al., 2009).

We probed for *sema5a* expression and found it is present in several regions of the zebrafish brain, most predominantly in the OB at 48 hpf, although no habenular expression was observed (Supplementary Figure B.4A-A'). Because Sema5a is a transmembrane ligand, we also analysed the expression of its putative receptor, Plexin B3 (Artigiani et al., 2004). At 48 hpf, *plexin B3* has a very strong expression in the lateral region of the presumptive habenula on both sides, possibly in the precursors of the ventral habenula (vHb) (Supplementary Figure B.4B-B'). As their expression might indicate a possible function of Sema5a/PlexinB3 in the dHb, we used the same MO as reported by Hilario and colleagues, a splice-blocking MO which induces the excision of exon 7 in the Sema domain, to check for defects in habenular asymmetry. Although several concentrations of the MO were tested, no disruptions of *kctd12.1* expression were observed in MO injected embryos at 4 dpf (data not shown). Despite this, it is important to note that complete splicing of all *sema5a* transcripts were never observed by Hilario and colleagues, indicating that residual effects of the non-spliced transcripts might still be sufficient for the protein to function. It is also possible that the injected MO was not able to effectively target *sema5a* transcripts at the late timepoint where they might be required to act on habenular asymmetry. Nevertheless, these results suggest that *sema5a* is not the mutated gene in *narcissus*.

Many studies have already provided valuable information on how L-R asymmetries arise in the zebrafish epithalamus. However, how these asymmetries are maintained and ultimately give rise to neuroanatomical asymmetries at later stages during development is yet largely unknown. What is the nature of the parapineal/lHb communication? What modulates asymmetric Wnt and Notch signalling? What are their downstream effectors and how do all these factors contribute to the asymmetric neurogenesis of habenular precursors? The work reported here and the future analysis of *nss* mutants will help provide answers to some of these and other questions. It will be critical to identify the genetic

mutation responsible for the mutant phenotype, but also the cellular and molecular mechanisms that lead to the development of the phenotype observed in *nss* mutants. Ultimately, the understanding on how L-R asymmetries develop in the zebrafish brain, how they modulate function and behaviour and how they evolved will, in the long run, provide valuable insights on human laterality and the defects associated with it, but perhaps most importantly, allow for a small yet important comprehension of the phenomenon of life.

Appendix A

Supplementary Material

A.1 BrdU cell counting ImageJ macro

When ran, the macro prompts for a file directory with the files to be processed (*PROCESSED*) and then for another where the files should be saved (*SAVING*). Inputs are .tiff files with nuclear staining on channel 3, BrdU staining on channel 2 and *kctd12.1* staining on channel 1.

In summary, the macro starts by creating a binary image of all channels separately, using the "watershed" function to correctly separate the nuclei in the nuclear staining channel. It then creates an image composed by the colocalized pixels from nuclear and BrdU channels using the image calculator function "AND" and counts the nuclei by means of the "3D Object Counter" ImageJ plugin (http://rsbweb.nih.gov/ij/plugins/track/objects.html), defining the total number of BrdU cells (*total*). Next, it creates another image composed of the colocalized pixels of every channel and counts the nuclei again using the same plugin and settings, thereby defining the *kctd12.1* positive nuclei (*inlov*).

Every count is registered in a log file (counted_log.txt) that is saved in the "*SAVING*" directory, along with a merge image of every processed file composed by the channels of BrdU (green), *kctd12.1* (magenta), total nuclei counted centroids (red) and *kctd12.1* positive nuclei counted centroids (white).

Macro is as follows:

```
dir = getDirectory("Choose a Directory to PROCESS");
list = getFileList(dir);
dir2 = getDirectory("Choose a Directory for SAVING");

setBatchMode(true); //runs in batch mode, remove during troubleshooting steps
for (f=0; f <list.length; f++) {
path = dir+list[f];
open(path);

t=getTitle();

t2= t +' counted.tif';

run("Colors...", "foreground=white background=black selection=yellow");
run("Set Measurements...", " mean centroid redirect=None decimal=6");
n0=nSlices;
h=getHeight();
w=getWidth();
getVoxelSize(width, height, depth, unit);
wi=width;
hei=height;
d=depth;
u=unit;
run("Split Channels");
selectWindow("C3-" + t); //Nuclear staining channel (Replace the channel numbers if yours are different)
id=getImageID();
selectImage(id);
rename("ti1");
ti1=getTitle();
run("Grays");
```

```
run("Gaussian Blur...", "sigma=1 stack");
run("Subtract Background...", "rolling=25 sliding stack");
run("Set Scale...", "distance=0 known=1 pixel=1 unit=pixel");
run("Enhance Contrast", "saturated=0.3 normalize normalize_all");
run("Remove Outliers...", "radius=3 threshold=0 which=Bright stack");
run("Remove Outliers...", "radius=2 threshold=0 which=Dark stack");
setAutoThreshold("Li dark stack");
run("Convert to Mask", "method=Li background=Dark");
run("Watershed", "stack");

selectWindow("C2-" + t); //BrdU staining channel
id=getImageID();
selectImage(id);
rename("ti2");
ti2=getTitle();
run("Duplicate...", "title=brdu duplicate");
brdu=getTitle();
selectImage(ti2);
run("Grays");
run("Despeckle", "stack");
run("Despeckle", "stack");
run("Gaussian Blur...", "sigma=1 stack");
run("Subtract Background...", "rolling=25 sliding stack");
run("Set Scale...", "distance=0 known=1 pixel=1 unit=pixel");
run("Enhance Contrast", "saturated=0.01 normalize normalize_all");
run("Remove Outliers...", "radius=5 threshold=0 which=Bright stack");
run("Remove Outliers...", "radius=4 threshold=0 which=Dark stack");
setAutoThreshold("Li black dark stack");
run("Convert to Mask", "method=Li background=Dark");
run("Open", "stack");
run("Remove Outliers...", "radius=10 threshold=0 which=Dark stack");

selectWindow("C1-" + t); //kctd12.1 staining channel
```

```
id=getImageID();
selectImage(id);
rename("ti3");
ti3=getTitle();
run("Duplicate...", "title=lov duplicate");
lov=getTitle();
selectImage(ti3);
run("Grays");
run("Despeckle", "stack");
run("Gaussian Blur...", "sigma=2 stack");
run("Subtract Background...", "rolling=100 sliding stack");
run("Enhance Contrast", "saturated=0.01 normalize normalize_all");
run("Set Scale...", "distance=0 known=1 pixel=1 unit=pixel");
run("Remove Outliers...", "radius=5 threshold=0 which=Bright stack");
run("Remove Outliers...", "radius=6 threshold=0 which=Dark stack");
setAutoThreshold("IsoData black dark stack");
run("Convert to Mask", "method=IsoData background=Dark");
run("Fill Holes", "stack");
run("Median...", "radius=17 stack");
run("Dilate", "stack");
run("Dilate", "stack");

imageCalculator("AND create stack", ti1, ti2);
id=getImageID();
selectImage(id);
rename("total");
total=getTitle();
run("Open", "stack");
run("Grays");

mo=1;
for (i=1; i<=nSlices; i++)
setSlice(i);
```

```
getStatistics(area, mean, min, max);
if (max>min)
run("Find Maxima...", "noise="+mo+" output=[Point Selection]");
run("Enlarge...", "enlarge=4");
run("Clear Outside", "slice");
}
run("Select None");
}

setVoxelSize(wi, hei, d, u);
run("Grays");
run("Despeckle", "stack");
run("3D object counter...", "threshold=1 slice=2 min.=100 max.=9437184 centroids summary");
run("8-bit");
setMinAndMax(0, 1);
run("Apply LUT", "stack");

imageCalculator("AND create stack", ti3, total);
id=getImageID();
selectImage(id);
rename("inlov");
inlov=getTitle();
run("Open", "stack");
run("Fill Holes", "stack");
run("Grays");

mo=1;
for (i=1; i<=nSlices; i++)
setSlice(i);
getStatistics(area, mean, min, max);
if (max>min)
run("Find Maxima...", "noise="+mo+" output=[Point Selection]");
```

```
run("Enlarge...", "enlarge=4");
run("Clear Outside", "slice");
}
run("Select None");
}

setVoxelSize(wi, hei, d, u);
run("Grays");
run("Despeckle", "stack");
run("3D object counter...", "threshold=1 slice=2 min.=100 max.=9437184 centroids summary");
run("8-bit");
setMinAndMax(0, 1);
run("Apply LUT", "stack");

selectWindow("inlov");
close();
selectWindow("total");
close();
selectWindow("ti1");
close();
selectWindow("ti2");
close();
selectWindow("ti3");
close();
selectWindow(brdu);
run("Grays");
run("Despeckle", "stack");
run("Despeckle", "stack");
selectWindow(lov);
run("Grays");
run("Despeckle", "stack");
selectWindow("Centroids map of inlov");
```

```
run("Grays");
selectWindow("Centroids map of total");
run("Grays");
run("Merge Channels...", "c1=[Centroids map of total] c2=["+brdu+"] c4=[Centroids
map of inlov] c6=["+lov+"]");

rename(t2);
saveAs("Tiff", dir2 + t2 + ".tif");
run("Close");
}

selectWindow("Log");
saveAs("Text", dir2 + "counted_log.txt");
```

Appendix B

Supplementary Figures

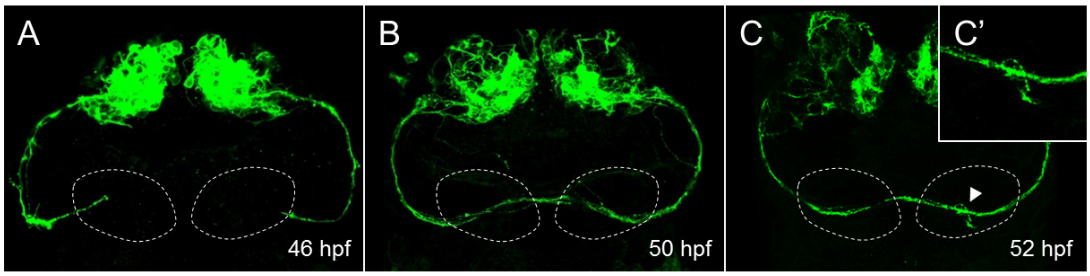

Figure B.1: **Timecourse analysis of Tg(lhx2a:gap-YFP) projections to the epithalamus. A,C',** The asymmetric projections to the right habenula nucleus from the olfactory bulb in Tg(lhx2a:gap-YFP) embryos starts to become apparent at 52 hpf (white arrowhead). The dotted lines represent the presumptive habenular nuclei.

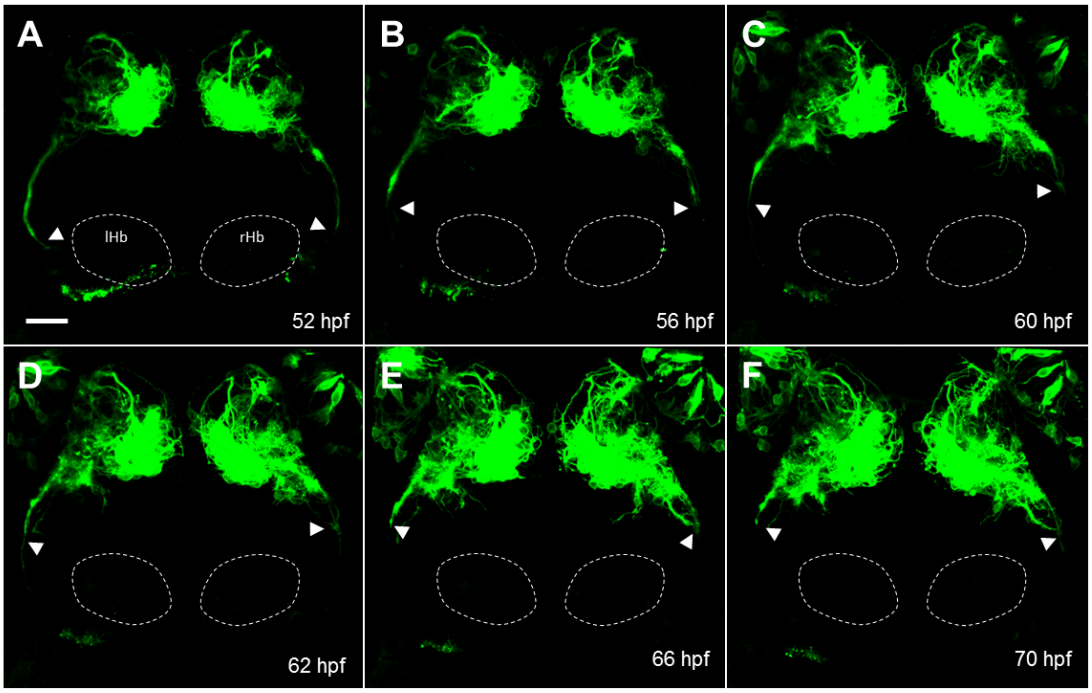

Figure B.2: **Axotomised lhx2a^{Tg+} axons degenerate back towards the olfactory bulb. A,F,** Frames from a timelapse movie recorded after left and right fasciculi of lhx2a^{Tg+} mitral cells had been axotomised at 50 hpf reveals that they regress back to the olfactory bulb until 70 hpf. Arrowheads indicate the tip of the axons. Dotted lines represent the presumptive habenular nuclei. rHb, Right habenula; lHb, Left habenula. Scale bar=25 μm.

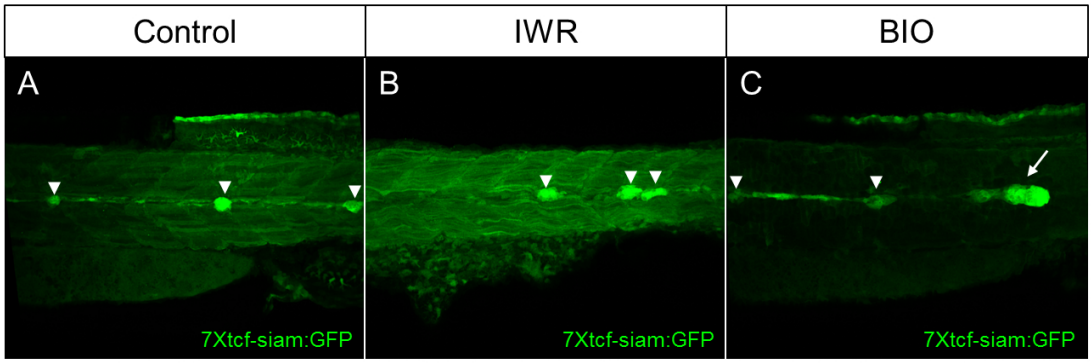

Figure B.3: **Pharmacological treatments disrupting Wnt signalling affect the development of the lateral line. A,** 1% DMSO control, **B,** IWR-1 and **C,** BIO treated Tg(7Xtcf-siam:GFP)^{ia4} embryos from 32–48 hpf and immunolabelled for the transgene expression. All embryos were fixed at 48 hpf. Arrowheads represent the neuromasts and the arrow in B indicates the lateral line primordium, which is stalled in this condition.

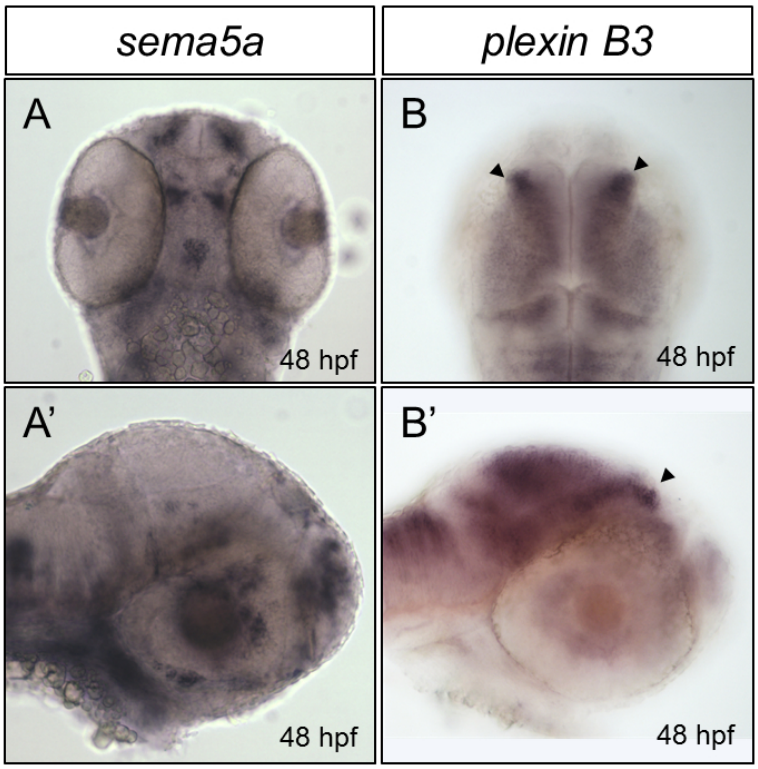

Figure B.4: **Expression of *sema5a* and its receptor *plexin B3* in the zebrafish brain. A-B',** Dorsal and lateral views of the expression pattern of **A-A',** *sema5a* and **B-B',** *plexin B3* in the brain of zebrafish at 48 hpf. Arrowheads indicate expression in the region of the epithalamus, in the presumptive habenulae nuclei.

References

Agetsuma, Masakazu; Aizawa, Hidenori; Aoki, Tazu; Nakayama, Ryoko; Takahoko, Mikako; Goto, Midori; Sassa, Takayuki; Amo, Ryunosuke; Shiraki, Toshiyuki; Kawakami, Koichi; Hosoya, Toshihiko; Higashijima, Shin-ichi, and Okamoto, Hitoshi. The habenula is crucial for experience-dependent modification of fear responses in zebrafish. *Nature neuroscience*, 13(11):1354–1356, 2010. 8

Aizawa, Hidenori. Habenula and the asymmetric development of the vertebrate brain. *Anatomical science international*, 2012. 7, 10

Aizawa, Hidenori; Bianco, Isaac; Hamaoka, Takanori; Miyashita, Toshio; Uemura, Osamu; Concha, Miguel; Russell, Claire; Wilson, Stephen, and Okamoto, Hitoshi. Laterotopic representation of left-right information onto the dorsoventral axis of a zebrafish midbrain target nucleus. *Current biology : CB*, 15 (3):238–243, 2005. 10, 41

Aizawa, Hidenori; Goto, Midori; Sato, Tomomi, and Okamoto, Hitoshi. Temporally regulated asymmetric neurogenesis causes left-right difference in the zebrafish habenular structures. *Developmental cell*, 12(1):87–98, 2007. 12, 34, 43, 44, 45

Alberi, Lavinia; Liu, Shuxi; Wang, Yue; Badie, Ramy; Constance, Smith-Hicks,; Wu, Jing; Pierfelice, Tarran; Abazyan, Bagrat; Mattson, Mark; Kuhl, Dietmar; Pletnikov, Mikhail; Worley, Paul, and Gaiano, Nicholas. Activity-induced notch signaling in neurons requires Arc/Arg3.1 and is essential for synaptic plasticity in hippocampal networks. *Neuron*, 69(3):437–444, 2011. 43

Amo, Ryunosuke; Aizawa, Hidenori; Takahoko, Mikako; Kobayashi, Megumi; Takahashi, Rieko; Aoki, Tazu, and Okamoto, Hitoshi. Identification of the zebrafish ventral habenula as a homolog of the mammalian lateral habenula. *The Journal of neuroscience : the official journal of the Society for Neuroscience*, 30(4):1566–1574, 2010. 9

Andres, Karl; von Düring, Monika, and Veh, Rüdiger. Subnuclear organization of the rat habenular complexes. *The Journal of comparative neurology*, 407(1): 130–150, 1999. 10

Artigiani, Stefania; Conrotto, Paolo; Fazzari, Pietro; Gilestro, Giorgio; Barberis, Davide; Giordano, Silvia; Comoglio, Paolo, and Tamagnone, Luca. Plexin-B3 is a functional receptor for semaphorin 5A. *EMBO reports*, 5(7):710–714, 2004. 46

Badcock, Nicholas; Bishop, Dorothy; Hardiman, Mervyn; Barry, Johanna, and Watkins, Kate. Co-localisation of abnormal brain structure and function in specific language impairment. *Brain and language*, 120(3):310–320, 2012. 5

Barth, K; Miklosi, Adam; Watkins, Jenny; Bianco, Isaac; Wilson, Stephen, and Andrew, Richard. fsi zebrafish show concordant reversal of laterality of viscera, neuroanatomy, and a subset of behavioral responses. *Current biology : CB*, 15 (9):844–850, 2005. 13

Bianco, Isaac and Wilson, Stephen. The habenular nuclei: a conserved asymmetric relay station in the vertebrate brain. *Philosophical transactions of the Royal Society of London. Series B, Biological sciences*, 364(1519):1005–1020, 2009. 7

Biemar, F; Argenton, F; Schmidtke, R; Epperlein, S; Peers, B, and Driever, W. Pancreas development in zebrafish: early dispersed appearance of endocrine hormone expressing cells and their convergence to form the definitive islet. *Developmental biology*, 230(2):189–203, 2001. 19

Bisazza, A; Rogers, L, and Vallortigara, G. The origins of cerebral asymmetry: a review of evidence of behavioural and brain lateralization in fishes, reptiles

and amphibians. *Neuroscience and biobehavioral reviews*, 22(3):411–426, 1998. 2

Bishop, Dorothy. Cerebral asymmetry and language development: cause, correlate, or consequence? *Science (New York, N.Y.)*, 340(6138), 2013. 5, 6

Broca, P. Sur le siège de la faculté du langage articulé dans l'hémisphère gauche du cerveau. *Bulletin de la Societe d'Anthmpologie*, 4:377–393, 1965. 2

Caldecott-Hazard, S; Mazziotta, J, and Phelps, M. Cerebral correlates of depressed behavior in rats, visualized using 14C-2-deoxyglucose autoradiography. *The Journal of neuroscience : the official journal of the Society for Neuroscience*, 8(6):1951–1961, 1988. 8

Carl, Matthias; Bianco, Isaac; Bajoghli, Baubak; Aghaallaei, Narges; Czerny, Thomas, and Wilson, Stephen. Wnt/Axin1/beta-catenin signaling regulates asymmetric nodal activation, elaboration, and concordance of CNS asymmetries. *Neuron*, 55(3):393–405, 2007. 10, 13

Carlson, J; Noguchi, K, and Ellison, G. Nicotine produces selective degeneration in the medial habenula and fasciculus retroflexus. *Brain research*, 906(1-2): 127–134, 2001. 8

Chen, Baozhi; Dodge, Michael; Tang, Wei; Lu, Jianming; Ma, Zhiqiang; Fan, Chih-Wei; Wei, Shuguang; Hao, Wayne; Kilgore, Jessica; Williams, Noelle; Roth, Michael; Amatruda, James; Chen, Chuo, and Lum, Lawrence. Small molecule-mediated disruption of wnt-dependent signaling in tissue regeneration and cancer. *Nature chemical biology*, 5(2):100–107, 2009. 38

Concha, M and Wilson, S. Asymmetry in the epithalamus of vertebrates. *Journal of anatomy*, 199(Pt 1-2):63–84, 2001. 6

Concha, M; Burdine, R; Russell, C; Schier, A, and Wilson, S. A nodal signaling pathway regulates the laterality of neuroanatomical asymmetries in the zebrafish forebrain. *Neuron*, 28(2):399–409, 2000. 10, 12, 24

Concha, Miguel; Russell, Claire; Regan, Jennifer; Tawk, Marcel; Sidi, Samuel; Gilmour, Darren; Kapsimali, Marika; Sumoy, Lauro; Goldstone, Kim; Amaya, Enrique; Kimelman, David; Nicolson, Teresa; Gründer, Stefan; Gomperts, Miranda; Clarke, Jonathan, and Wilson, Stephen. Local tissue interactions across the dorsal midline of the forebrain establish CNS laterality. *Neuron*, 39(3): 423–438, 2003. 42

Concha, Miguel; Signore, Iskra, and Colombo, Alicia. Mechanisms of directional asymmetry in the zebrafish epithalamus. *Seminars in cell & developmental biology*, 20(4):498–509, 2009. 14

Concha, Miguel; Bianco, Isaac, and Wilson, Stephen. Encoding asymmetry within neural circuits. *Nature reviews. Neuroscience*, 13(12):832–843, 2012. 11

Corballis, Michael. The evolution and genetics of cerebral asymmetry. *Philosophical transactions of the Royal Society of London. Series B, Biological sciences*, 364(1519):867–879, 2009. 1

de Borsetti, Nancy; Dean, Benjamin; Bain, Emily; Clanton, Joshua; Taylor, Robert, and Gamse, Joshua. Light and melatonin schedule neuronal differentiation in the habenular nuclei. *Developmental biology*, 358(1):251–261, 2011. 18

Doll, Caleb; Burkart, Jarred; Hope, Kyle; Halpern, Marnie, and Gamse, Joshua. Subnuclear development of the zebrafish habenular nuclei requires ER translocon function. *Developmental biology*, 360(1):44–57, 2011. 41, 44

Frasnelli, Elisa; Vallortigara, Giorgio, and Rogers, Lesley. Left-right asymmetries of behaviour and nervous system in invertebrates. *Neuroscience and biobehavioral reviews*, 36(4):1273–1291, 2012. 1

Gamse, Joshua; Shen, Yu-Chi; Thisse, Christine; Thisse, Bernard; Raymond, Pamela; Halpern, Marnie, and Liang, Jennifer. Otx5 regulates genes that show circadian expression in the zebrafish pineal complex. *Nature genetics*, 30(1): 117–121, 2002. 15

Gamse, Joshua; Thisse, Christine; Thisse, Bernard, and Halpern, Marnie. The parapineal mediates left-right asymmetry in the zebrafish diencephalon. *Development (Cambridge, England)*, 130(6):1059–1068, 2003. 10, 13, 28, 42

Gamse, Joshua; Kuan, Yung-Shu; Macurak, Michelle; Brösamle, Christian; Thisse, Bernard; Thisse, Christine, and Halpern, Marnie. Directional asymmetry of the zebrafish epithalamus guides dorsoventral innervation of the midbrain target. *Development (Cambridge, England)*, 132(21):4869–4881, 2005. 9, 10, 19

Gazzaniga, Michael. Forty-five years of split-brain research and still going strong. *Nature reviews. Neuroscience*, 6(8):653–659, 2005. 2

Geisler, Stefanie; Andres, Karl, and Veh, Rüdiger. Morphologic and cytochemical criteria for the identification and delineation of individual subnuclei within the lateral habenular complex of the rat. *The Journal of comparative neurology*, 458(1):78–97, 2003. 10

Geschwind, N and Levitsky, W. Human brain: left-right asymmetries in temporal speech region. *Science (New York, N.Y.)*, 161(3837):186–187, 1968. 2

Good, C; Johnsrude, I; Ashburner, J; Henson, R; Friston, K, and Frackowiak, R. A voxel-based morphometric study of ageing in 465 normal adult human brains. *NeuroImage*, 14(1 Pt 1):21–36, 2001. 2

Gurusinghe, C; Zappia, J, and Ehrlich, D. The influence of testosterone on the sex-dependent structural asymmetry of the medial habenular nucleus in the chicken. *Journal of Comparative Neurology*, 253(2):153–162, 1986. 9

Her, Guor; Chiang, Chia-Chang; Chen, Wen-Ya, and Wu, Jen-Leih. In vivo studies of liver-type fatty acid binding protein (L-FABP) gene expression in liver of transgenic zebrafish (Danio rerio). *FEBS letters*, 538(1-3):125–133, 2003. 19

Hikosaka, Okihide. The habenula: from stress evasion to value-based decision-making. *Nature reviews. Neuroscience*, 11(7):503–513, 2010. 7, 8

Hilario, Jona; Louise, Rodino-Klapac,; Wang, Chunping, and Beattie, Christine. Semaphorin 5A is a bifunctional axon guidance cue for axial motoneurons in vivo. *Developmental biology*, 326(1):190–200, 2009. 19, 46

Hiscock, M; Inch, R; Jacek, C; Hiscock-Kalil, C, and Kalil, K. Is there a sex difference in human laterality? i. an exhaustive survey of auditory laterality studies from six neuropsychology journals. *Journal of clinical and experimental neuropsychology*, 16(3):423–435, 1994. 2

Hobert, Oliver; Johnston, Robert, and Chang, Sarah. Left-right asymmetry in the nervous system: the caenorhabditis elegans model. *Nature reviews. Neuroscience*, 3(8):629–640, 2002. 1

Kantor, David; Chivatakarn, Onanong; Peer, Katherine; Oster, Stephen; Inatani, Masaru; Hansen, Michael; Flanagan, John; Yamaguchi, Yu; Sretavan, David; Giger, Roman, and Kolodkin, Alex. Semaphorin 5A is a bifunctional axon guidance cue regulated by heparan and chondroitin sulfate proteoglycans. *Neuron*, 44(6):961–975, 2004. 45

Kertesz, A; Black, S; Polk, M, and Howell, J. Cerebral asymmetries on magnetic resonance imaging. *Cortex; a journal devoted to the study of the nervous system and behavior*, 22(1):117–127, 1986. 2

Kishimoto, Norihito; Asakawa, Kazuhide; Madelaine, Romain; Blader, Patrick; Kawakami, Koichi, and Sawamoto, Kazunobu. Interhemispheric asymmetry of olfactory input-dependent neuronal specification in the adult brain. *Nature neuroscience*, 16(7):884–888, 2013. 13, 43

Knecht, S; Deppe, M; Ringelstein, E; Wirtz, M; Lohmann, H; Dräger, B; Huber, T, and Henningsen, H. Reproducibility of functional transcranial doppler sonography in determining hemispheric language lateralization. *Stroke; a journal of cerebral circulation*, 29(6):1155–1159, 1998. 5

Kos, Miriam; van den Brink, Danielle; Snijders, Tineke; Rijpkema, Mark; Franke, Barbara; Fernandez, Guillen, and Hagoort, Peter. CNTNAP2 and language processing in healthy individuals as measured with ERPs. *PloS one*, 7(10), 2012. 6

Kuan, Yung-Shu; Yu, Hung-Hsiang; Moens, Cecilia, and Halpern, Marnie. Neuropilin asymmetry mediates a left-right difference in habenular connectivity. *Development (Cambridge, England)*, 134(5):857–865, 2007. 24

Levy, Jerre. The mammalian brain and the adaptive advantage of cerebral asymmetry. *Annals of the New York Academy of Sciences*, 299, 1977. 5

Li, Kun; Zhou, Tao; Liao, Lujian; Yang, Zhongfei; Wong, Catherine; Henn, Fritz; Malinow, Roberto; Yates, John, and Hu, Hailan. CaMKII in lateral habenula mediates core symptoms of depression. *Science (New York, N.Y.)*, 341(6149): 1016–1020, 2013. 8

Liang, J; Etheridge, A; Hantsoo, L; Rubinstein, A; Nowak, S; Izpisúa Belmonte, J, and Halpern, M. Asymmetric nodal signaling in the zebrafish diencephalon positions the pineal organ. *Development (Cambridge, England)*, 127(23):5101–5112, 2000. 10

Lieber, Toby; Kidd, Simon, and Struhl, Gary. DSL-Notch signaling in the drosophila brain in response to olfactory stimulation. *Neuron*, 69(3):468–481, 2011. 43

Lippolis, Giuseppe; Bisazza, Angelo; Rogers, Lesley, and Vallortigara, Giorgio. Lateralisation of predator avoidance responses in three species of toads. *Laterality*, 7(2):163–183, 2002. 2

Long, Sarah; Ahmad, Nadira, and Rebagliati, Michael. The zebrafish nodal-related gene southpaw is required for visceral and diencephalic left-right asymmetry. *Development (Cambridge, England)*, 130(11):2303–2316, 2003. 10

Macdonald, Rachel. Zebrafish immunohistochemistry. *Methods in Molecular Biology*, 127:77–88, 1999. 19

Matsumoto, Masayuki and Hikosaka, Okihide. Lateral habenula as a source of negative reward signals in dopamine neurons. *Nature*, 447(7148):1111–1115, 2007. 8

Meijer, Laurent; Skaltsounis, Alexios-Leandros; Magiatis, Prokopios; Polychronopoulos, Panagiotis; Knockaert, Marie; Leost, Maryse; Ryan, Xiaozhou; Vonica, Claudia; Brivanlou, Ali; Dajani, Rana; Crovace, Claudia; Tarricone, Cataldo; Musacchio, Andrea; Roe, S; Pearl, Laurence, and Greengard, Paul. GSK-3-selective inhibitors derived from tyrian purple indirubins. *Chemistry & biology*, 10(12):1255–1266, 2003. 38

Miklósi, A and Andrew, R. Right eye use associated with decision to bite in zebrafish. *Behavioural brain research*, 105(2):199–205, 1999. 13

Miklósi, A; Andrew, R, and Savage, H. Behavioural lateralisation of the tetrapod type in the zebrafish (Brachydanio rerio). *Physiology & behavior*, 63(1):127–135, 1997. 4, 13

Miklósi, A; Andrew, R, and Gasparini, S. Role of right hemifield in visual control of approach to target in zebrafish. *Behavioural brain research*, 122(1):57–65, 2001. 4

Miyasaka, Nobuhiko; Morimoto, Kozo; Tsubokawa, Tatsuya; Higashijima, Shinichi; Okamoto, Hitoshi, and Yoshihara, Yoshihiro. From the olfactory bulb to higher brain centers: genetic visualization of secondary olfactory pathways in zebrafish. *The Journal of neuroscience : the official journal of the Society for Neuroscience*, 29(15):4756–4767, 2009. 28

Nawabi, Homaira and Castellani, Valérie. Axonal commissures in the central nervous system: how to cross the midline? *Cellular and molecular life sciences : CMLS*, 68(15):2539–2553, 2011. 24

Nestor, P and Safer, M. A multi-method investigation of individual differences in hemisphericity. *Cortex; a journal devoted to the study of the nervous system and behavior*, 26(3):409–421, 1990. 4

Pinel, Philippe; Fauchereau, Fabien; Moreno, Antonio; Barbot, Alexis; Lathrop, Mark; Zelenika, Diana; Le Bihan, Denis; Poline, Jean-Baptiste; Bourgeron, Thomas, and Dehaene, Stanislas. Genetic variants of FOXP2 and

KIAA0319/TTRAP/THEM2 locus are associated with altered brain activation in distinct language-related regions. *The Journal of neuroscience : the official journal of the Society for Neuroscience*, 32(3):817–825, 2012. 6

Rasband, W. Imagej. , 1997. National Institutes of Health, Bethesda, Maryland, USA. 22

Raya, Angel; Kawakami, Yasuhiko; Concepcion, Rodriguez-Esteban,; Buscher, Dirk; Koth, Christopher; Itoh, Tohru; Morita, Masanobu; Raya, R; Dubova, Ilir; Bessa, Joaquin; de la Pompa, Jose, and Izpisua Belmonte, Juan. Notch activity induces nodal expression and mediates the establishment of left-right asymmetry in vertebrate embryos. *Genes & development*, 17(10):1213–1218, 2003. 12

Raya, Angel; Kawakami, Yasuhiko; Concepción, Rodríguez-Esteban,; Ibañes, Marta; Diego, Rasskin-Gutman,; Joaquín, Rodríguez-León,; Büscher, Dirk; Feijó, José, and Izpisúa Belmonte, Juan. Notch activity acts as a sensor for extracellular calcium during vertebrate left-right determination. *Nature*, 427 (6970):121–128, 2004. 12

Regan, Jennifer; Concha, Miguel; Roussigne, Myriam; Russell, Claire, and Wilson, Stephen. An fgf8-dependent bistable cell migratory event establishes CNS asymmetry. *Neuron*, 61(1):27–34, 2009. 13

Rogers, Lesley; Zucca, Paolo, and Vallortigara, Giorgio. Advantages of having a lateralized brain. *Proceedings. Biological sciences / The Royal Society*, 271 Suppl 6:S420–S422, 2004. 5

Roussigné, Myriam; Bianco, Isaac; Wilson, Stephen, and Blader, Patrick. Nodal signalling imposes left-right asymmetry upon neurogenesis in the habenular nuclei. *Development (Cambridge, England)*, 136(9):1549–1557, 2009. 12, 35

Salas, Ramiro; Sturm, Renea; Boulter, Jim, and De Biasi, Mariella. Nicotinic receptors in the habenulo-interpeduncular system are necessary for nicotine withdrawal in mice. *The Journal of neuroscience : the official journal of the Society for Neuroscience*, 29(10):3014–3018, 2009. 8

Shepard, Jennifer; Stern, Howard; Pfaff, Kathleen, and Amatruda, James. Analysis of the cell cycle in zebrafish embryos. *Methods in cell biology*, 76:109–125, 2004. 20

Shumake, J; Edwards, E, and F, Gonzalez-Lima,. Opposite metabolic changes in the habenula and ventral tegmental area of a genetic model of helpless behavior. *Brain research*, 963(1-2):274–281, 2003. 8

Tamotsu, S; Korf, H; Morita, Y, and Oksche, A. Immunocytochemical localization of serotonin and photoreceptor-specific proteins (rod-opsin, s-antigen) in the pineal complex of the river lamprey, lampetra japonica, with special reference to photoneuroendocrine cells. *Cell and tissue research*, 262(2):205–216, 1990. 6

Thisse, Christine and Thisse, Bernard. High-resolution in situ hybridization to whole-mount zebrafish embryos. *Nature protocols*, 3(1):59–69, 2008. 19

Toga, Arthur and Thompson, Paul. Mapping brain asymmetry. *Nature reviews. Neuroscience*, 4(1):37–48, 2003. 3

Turner, Katherine; Bracewell, Thomas, and Hawkins, Thomas. Anatomical dissection of zebrafish brain development. *Methods in Molecular Biology*, 1082: 197–214, 2014. 20

Ullsperger, Markus and von Cramon, D. Error monitoring using external feedback: specific roles of the habenular complex, the reward system, and the cingulate motor area revealed by functional magnetic resonance imaging. *The Journal of neuroscience : the official journal of the Society for Neuroscience*, 23(10):4308–4314, 2003. 8

Valdivia, Leonardo; Young, Rodrigo; Hawkins, Thomas; Stickney, Heather; Cavodeassi, Florencia; Schwarz, Quenten; Pullin, Lisa; Villegas, Rosario; Moro, Enrico; Argenton, Francesco; Allende, Miguel, and Wilson, Stephen. Lef1-dependent wnt/β-catenin signalling drives the proliferative engine that maintains tissue homeostasis during lateral line development. *Development (Cambridge, England)*, 138(18):3931–3941, 2011. 39

Vallortigara, G. Comparative neuropsychology of the dual brain: a stroll through animals' left and right perceptual worlds. *Brain and language*, 73(2):189–219, 2000. 5

Vallortigara, G and Andrew, R. Lateralization of response by chicks to change in a model partner. *Animal Behaviour*, 41(2):184–194, 1991. 5

Vallortigara, Giorgio and Rogers, Lesley. Survival with an asymmetrical brain: advantages and disadvantages of cerebral lateralization. *The Behavioral and brain sciences*, 28(4):575–89; discussion 589, 2005. 1, 2, 4

Wallman, J and Pettigrew, J. Conjugate and disjunctive saccades in two avian species with contrasting oculomotor strategies. *The Journal of neuroscience : the official journal of the Society for Neuroscience*, 5(6):1418–1428, 1985. 5

Westerfield, Monte. *The zebrafish book. A guide for the laboratory use of zebrafish (Danio rerio)*. Univ. of Oregon Press, Eugene, 2000. 18

Wolman, David. The split brain: a tale of two halves. *Nature*, 483(7389):260–263, 2012. 2

Wree, A; Zilles, K, and Schleicher, A. Growth of fresh volumes and spontaneous cell death in the nuclei habenulae of albino rats during ontogenesis. *Anatomy and embryology*, 161(4):419–431, 1981. 9

Wurtman, R; Axelrod, J, and Fisher, J. Melatonin synthesis in the pineal gland: effect of light mediated by the sympathetic nervous system. *Science*, 143(3612): 1328–1330, 1964. 6

Zilles, K; Schleicher, A, and Wingert, F. Quantitative growth analysis of limbic nuclei areas fresh volume in diencephalon and mesencephalon of an albino mouse ontogenic series. i. nucleus habenulare. *Journal für Hirnforschung*, 17 (1):1–10, 1976. 9